Title

Network-wide abnormalities explain memory variability in hippocampal amnesia

Authors' Names

Georgios P. D. Argyropoulos PhD [1]

Clare Loane PhD [1,2]

Adriana Roca-Fernandez MSc [1]

Carmen Lage-Martinez MD [1,3]

Oana Gurau MSc [1]

Sarosh R Irani FRCP, PhD [4]

Christopher R Butler FRCP, PhD [1]

Affiliations

[1] Memory Research Group, Nuffield Department of Clinical Neurosciences, University of Oxford, Oxford, UK.

[2] Institute of Cognitive Neuroscience, University College London, London, UK.

[3] Valdecilla Biomedical Research Institute, University Hospital Marqués de Valdecilla.

[4] Oxford Autoimmune Neurology Group, Nuffield Department of Clinical Neurosciences, University of Oxford, Oxford, UK.

Corresponding author: Georgios P. D. Argyropoulos; georgios.argyropoulos@ndcn.ox.ac.uk; Medical Sciences Division, Nuffield Department of Clinical Neurosciences, Level 6, West Wing, John Radcliffe Hospital, Oxford, OX3 9DU, UK.

Abstract

Patients with hippocampal amnesia play a central role in memory neuroscience but the neural underpinnings of amnesia are hotly debated. We hypothesized that focal hippocampal damage is associated with changes across the extended hippocampal system and that these, rather than hippocampal atrophy per se, would explain variability in memory between patients. We assessed this hypothesis in a uniquely large cohort of patients (n=38) after autoimmune limbic encephalitis, a syndrome associated with focal structural hippocampal pathology. These patients showed impaired recall, recognition and maintenance of new information, and remote autobiographical amnesia. Besides hippocampal atrophy, we observed correlatively reduced thalamic volume, resting-state inter-hippocampal connectivity and activity in posteromedial cortex. Associations of hippocampal volume with recall, recognition, and remote memory were fully mediated by wider network abnormalities, and were only direct in forgetting. Such network abnormalities may explain the variability across studies of amnesia and speak to theoretical debates in memory neuroscience.

Introduction

Ever since the first report of the famous patient H.M. (Scoville and Milner, 1957), hippocampal (HPC) amnesia has played a fundamental role in the neuroscience of human memory. Studies of amnesic patients have, however, often produced inconsistent results. Such studies have been criticized for attributing behavioral deficits solely to the HPC (Squire and Wixted, 2011), despite the fact that focal damage may trigger more subtle structural and functional abnormalities across an extended HPC system (Aggleton, 2014). Indeed, broader network abnormalities are well documented in other 'focal' conditions [e.g. ischemic stroke (Carter et al., 2009; Veldsman et al., 2018)] and have been demonstrated in small case series of amnesic patients (Hayes et al., 2012; Henson et al., 2016; Rudebeck et al., 2013). While these abnormalities may be important in understanding memory impairment in neurological disease (Addis et al., 2007), their explanatory potential is under-explored.

We propose that network abnormalities are key to understanding inconsistencies underpinning central debates about HPC function in amnesia research. One such debate centers on the dissociation of neurocognitive processes underlying recall and recognition. Some authors hold that recall relies on HPC-dependent recollection processes, whereas recognition additionally draws on familiarity, which is mediated by non-HPC structures within the medial temporal lobe (MTL) (Brown and Aggleton, 2001; Kafkas et al., 2016). Others argue that recollection and familiarity do not dissociate within the MTL (Wixted and Squire, 2010). A second debate concerns the material-specificity of HPC processing. According to some theorists, the HPC has a privileged role in processing scenes or spatial stimuli and this function underpins its involvement in

episodic memory and navigation (Maguire and Mullally, 2013, Graham et al., 2010). An opposing view holds that the primary role of the HPC is the material-independent maintenance of information over a limited time period (Kim et al., 2015). A third debate pertains to the HPC role in remote memory. The 'standard consolidation theory' holds that newly-acquired memories initially depend upon the HPC but that, through a process of 'consolidation', memory traces gradually become HPC-independent and are stored in and retrieved by neocortical structures alone (Hardt and Nadel, 2018; Squire et al., 2015). In contrast, 'multiple trace theory' proposes that the HPC is necessary for vivid episodic recollection irrespective of the age of the memory (Moscovitch et al., 2005).

A central problem for addressing these debates with neuropsychology and, more specifically, for determining the relevance of wider brain network abnormalities, is that HPC amnesia is very rare. Consequently, most studies rely upon just a handful of amnesic cases and are thus susceptible to confounds such as impairment severity, measurement noise and individual differences (Lambon Ralph et al., 2011, 2002). Larger cohort studies would partially overcome these confounds and capitalize on case heterogeneity to map behavior to brain structure and function.

In order to explore the impact of HPC damage on wider brain networks and determine the impact of these abnormalities upon memory, we studied a uniquely large cohort (n=38) of patients after autoimmune limbic encephalitis (LE). In its acute phase, this highly consistent clinical syndrome classically causes focal HPC damage, seen on MRI as high T2 signal (Finke et al., 2017; Kotsenas et al., 2014). Although most patients respond well to early immunosuppressive therapy (Finke et al., 2017; Irani et al., 2011;

89 Thompson et al., 2018), some subsequently develop HPC atrophy and persistent
90 cognitive impairment, the most prominent aspect of which is anterograde amnesia
91 (Butler et al., 2014; Finke et al., 2017; Irani et al., 2013; Malter et al., 2014).
92 Autoimmune LE patients are a key group in studies of HPC amnesia (Hassabis et al.,
93 2007; Henson et al., 2017, 2016; Maguire et al., 2006). Post-mortem studies
94 demonstrate focal HPC damage (Khan et al., 2009; Park et al., 2007), contrasting with
95 the wider damage typically found following other encephalitides [e.g. herpes simplex
96 encephalitis (Damasio and Van Hoesen, 1985; Gitelman et al., 2001)] or global
97 ischemia/anoxia (Huang and Castillo, 2008), conditions that have also been used as
98 models of human HPC function [for discussion, see (Squire and Zola, 1996)]. Patients'
99 varying degrees of residual symptom severity offered us the opportunity to examine the
100 relationships between cognition and brain structure and function.
101
102 Patients (n=38) and healthy controls (n=41) were assessed with a thorough battery of
103 neuropsychological tests of episodic memory (for verbal and visual material) and other
104 cognitive functions, in order to identify the tasks in which patients showed impaired
105 performance. The tests we employed are robust, widely used, well-normed, and largely
106 model-free (see below). Using manual volumetry of MTL regions, as well as whole-
107 brain, voxel-based investigations of structural MRI and resting-state fMRI, we identified
108 the differences in brain structure and function between patients and controls. Finally,
109 we investigated the relationship between brain abnormalities and cognitive deficits. We
110 predicted that i) focal HPC damage would be accompanied by remote abnormalities in
111 the extended HPC system; ii) variation in the extent of these network-wide
112 abnormalities across patients would explain variability in anterograde and retrograde

113 memory impairment; iii) taking into account these abnormalities would help identify
114 which particular aspects of memory impairment are a direct function of HPC atrophy.

Results

Neuropsychological Assessment

The patients included in this study (n=38) had been diagnosed with autoimmune LE, and were recruited post-acutely, after reassessment by an experienced neurologist (CRB) prior to study inclusion (see Methods).

Patients did not differ from controls (n=41; matched for age and M:F ratio) in premorbid intelligence, semantic memory and language, visuomotor and executive function. Their cognitive profile was characterized by highly focal episodic memory impairment. Patients were impaired in both recall and recognition of both verbal and visual material (including scenes), and showed pronounced forgetting of visual material – verbal forgetting was only marginally impaired. A clear exception was patients' preserved face recognition memory. They also showed impaired remote autobiographical memory for both childhood and early adulthood epochs, but preserved remote personal semantic memory. Although they showed higher scores on the depression sub-scale of the Hospital Anxiety and Depression Scale (Zigmond and Snaith, 1983), the median score was well below the clinical cut-off, and none of the patients scored within the severe range (mild range: 3 patients; moderate range: 4 patients; non-case range: rest of patients and all controls) (table 1).

[table 1]

For further correlational analyses, and in order to minimize the probability of measurement error and maximize the generalizability of our findings, we derived 6 composite memory scores per participant. These comprised scores on individual tests in which patients showed impaired performance at group level compared with controls: composite scores for verbal recall, verbal recognition, visual recall, visual recognition and visual forgetting were derived by averaging the corresponding standardized age-scaled scores; a remote autobiographical memory score was calculated by summing the scores on autobiographical memories for childhood and early adulthood epochs (table S1).

None of those composite memory scores correlated with scores for depression (HADS) across patients (all rhos, |rho| < 0.19; all ps, p-unc > 0.3), except for visual forgetting at uncorrected levels (rho=-0.425, p-unc=0.015). In the following analyses, we thus also examined the relationship among visual forgetting, its structural and functional correlates, and scores for depression across patients.

Structural Abnormalities

Volumetry

The volumes of MTL and other subcortical structures were corrected for total intra-cranial volume (TIV) and expressed as z scores based on the mean volume and SD of individually age-matched controls for each patient (see Methods). Consistent with the neuroradiological reports on patients' acute clinical T2-weighted MRI scans (table 5) and the fact that acute HPC T2 hyperintensity and swelling are followed by post-acute HPC atrophy in LE (Finke et al., 2017; Irani et al., 2013), the volumetric analysis of

patients' post-acute MRIs disclosed HPC atrophy (one-sample t-test: volume (z) vs -1.5 SD: t=-2.17, p=0.037). Even at a lower threshold (vs. -1 SD), no other structure showed group-level atrophy (tables 2; S2). The right HPC showed more extensive atrophy (mean(z)=-2.38; SD(z)=2.13) than the left (mean(z)=-1.86; SD(z)=2.01; t=-2.086, p=0.044).

[table 2]

Whole-brain VBM: GM volume

Patients showed bilateral volume reduction in the HPC and the anterior, mediodorsal, and dorsolateral regions of the thalamus (figure 1a; table 3).

[table 3]

Resting-state Hemodynamic Activity

Patients showed reduced resting-state amplitude of low frequency fluctuations (rsALFF) in the posterior cingulate cortex (PCC) and the precuneus (figure 1b-c).

Resting-state Functional Connectivity

Voxel-to-Voxel rsFC: MVPA

In order to identify, in a data-driven fashion, regions in patients that show abnormal resting-state functional connectivity (rsFC) with the rest of the brain, we conducted a

whole-brain, voxel-to-voxel multivariate pattern analysis (MVPA) contrasting controls' and patients' rsFC for each voxel. This analysis showed group differences in the rsFC of a right HPC cluster (figure 1d).

Seed-to-Voxel rsFC

The right HPC was thus selected as a seed region for a whole-brain seed-to-voxel rsFC analysis, in order to identify specific regions that showed reduced HPC rsFC in patients. The spatially unsmoothed timeseries data were extracted from participants' manually delineated right HPC in native space, ensuring that rsFC differences were not an artefact of insufficient co-registration of the atrophic HPC. This seed region showed reduced rsFC with clusters in the medial prefrontal and posteromedial (PCC, retrosplenial, and precuneus) cortices, and the left HPC (figure 1e-g). We also wanted to ensure that the left HPC cluster that showed reduced rsFC with the right HPC was not a result of suboptimal co-registration of the functional images with the atrophic HPC. We thus used the mean rsFC values between the right and left HPC in native space (unsmoothed time series) instead of the left HPC cluster.

[figure 1]

Structure/Function-Behavior Correlations

Having identified the core brain abnormalities in our patient group, we investigated the contributions of these in explaining memory impairment.

Anterograde memory: Verbal Recognition

Correlations of verbal recognition memory scores with HPC GM volume (VBM clusters) across patients were only observed at uncorrected levels (average volume: r=0.391, p-unc=0.017; right HPC: r=0.340, p-unc=0.039; left HPC: r=0.388, p-unc=0.018; figure 2a; table S3). Marginal-to-moderate correlations were also observed with manually delineated HPC volumes (total HPC: r=0.285, p-unc=0.088; left: r=0.219, p-unc=0.192; right: r=0.354, p-unc=0.032; left anterior: r=0.333, p-unc=0.044; rest of rs, r < 0.32; rest of ps, p-unc > 0.06; table S4). However, verbal recognition scores correlated with patients' reduced inter-HPC rsFC (r=0.451, p-corr=0.049; figure 2b; table S3), which did not correlate with HPC volumes (VBM clusters, manually delineated volumes: all rs, r < 0.24; all ps, p-unc > 0.18). We thus entered mean inter-HPC rsFC and one of the six HPC volume measures as independent variables in six separate multiple step-wise linear regressions, with verbal recognition scores as the dependent variable. In all six analyses, the regression terminated in a single step, with inter-HPC rsFC as the only predictor of patients' performance (R^2=0.20; β(z)=0.451; F=8.18, p=0.007).

Interestingly, inter-HPC rsFC decreased across patients as a function of the delay between symptom onset and research scan (rho=-0.578, p-corr=0.002) (Table S5; figure 2c). No other brain abnormalities showed this relationship (all rhos, |rho| < 0.3; all ps, p-unc > 0.07).

[figure 2]

Anterograde memory: Visual Recognition

Visual recognition scores correlated across patients with their average HPC GM volume (r=0.427, p-corr=0.045), driven by the left HPC GM volume (r=0.433, p-unc=0.008; Table S3). However, they also correlated with reduced PCC rsALFF (r=0.543, p-corr=0.007). Left HPC GM volume correlated strongly with PCC rsALFF (r=0.412, p=0.014). The effects of left HPC GM volume reduction on visual recognition scores were fully mediated by the reduction in PCC rsALFF (figure 3).

Likewise, these scores correlated with manually delineated HPC volumes (total volume: r=0.332, p-unc=0.048), driven by the right HPC (r=0.438, p-unc=0.007; Table S4). Mean PCC rsALFF also correlated with the right HPC volume (r=0.529, p=0.001). The effects of right HPC atrophy on visual recognition were fully mediated by the reduction in PCC rsALFF (indirect effect: β=0.127, 95% CI: 0.053, 0.233; direct effect: β=0.114, p=0.252).

Given the reciprocal connectivity of thalamic nuclei with both the HPC and the posteromedial cortex (Aggleton, 2014; Aggleton et al., 2010) we assumed a causal chain of events, whereby focal HPC damage has remote effects on thalamic volume, which, in turn, leads to the functional abnormalities observed here in the PCC. A mediation analysis supported this hypothesis (figure S1).

[figure 3]

Anterograde memory: Verbal Recall

Verbal recall memory composite scores correlated across patients with their reduced PCC rsALFF (r=0.573, p-corr=0.003) and HPC GM volume (average: r=0.436, p-corr=0.036; left HPC: r=0.481, p-unc=0.003; right HPC: r=0.327, p-unc=0.048). The effects of HPC atrophy on verbal recall were fully mediated by the reduction in PCC rsALFF (figure 4). None of the manually delineated HPC volumes (total, left/right, anterior/posterior) correlated with verbal recall (all rs, r < 0.31; all ps, p-unc > 0.06).

[figure 4]

Anterograde memory: Visual Recall

Visual recall scores marginally correlated with PCC rsALFF (r=0.445, p-corr=0.056; table S3), and correlation with HPC GM cluster volumes was only noted at uncorrected and marginal levels (r=0.310, p-unc=0.066), driven by that with the left HPC volume (r=0.334, p-unc=0.046). The effects of HPC atrophy on visual recall were fully mediated by the reduction in PCC rsALFF (figure 5).

Of the manually delineated HPC volumes, only the right HPC correlated at uncorrected levels with visual recall (r=0.334, p-unc=0.047; table S4). The right HPC volumes correlated with patients' reduced PCC rsALFF (r=0.529, p=0.001). The effect of right HPC atrophy on visual recall was fully mediated by the reduction in PCC rsALFF (direct effect: β=0.076, p=0.53; indirect effect: β=0.126, 95% CI: 0.017, 0.262).

[figure 5]

Anterograde memory: Maintenance (Forgetting)

Visual forgetting scores correlated only with HPC GM volume (rho=0.546, p-corr=0.006; rest: p-corr > 0.14; table S3). This was driven by the correlation with the right HPC GM volume (rho=0.569, p-unc=0.0004; left: rho=0.410, p-unc=0.019). Correlations of visual forgetting with non-HPC abnormalities were only found at uncorrected levels (PCC rsALFF: rho=0.399, p-unc=0.024; table S3). PCC rsALFF correlated with right HPC GM volume (r=0.475, p=0.004). A mediation analysis demonstrated a direct effect of right HPC atrophy on visual forgetting scores (figure 6).

Similarly, visual forgetting scores correlated with all manually delineated HPC volumes (all rhos, rho > 0.375; all ps, p-unc < 0.03; table S4). The correlation was driven by the right HPC volume (rho=0.540, p-unc=0.001). The right HPC volume correlated with PCC rsALFF across patients (r=0.529, p=0.001). A mediation analysis demonstrated a direct effect of right HPC atrophy on visual forgetting scores (β=0.216, p=0.038; indirect effect: β=0.050, 95% CI: -0.057, 0.153).

Given that patients' depression (HADS) scores correlated with their visual forgetting scores, we examined their relationship with HPC atrophy. No correlation with HPC volumes (VBM clusters, manually delineated volumes) reached significance (all rhos, |rho| < 0.3; all ps, p-unc > 0.09), and right HPC volumes correlated with visual forgetting

scores over and above depression scores (GM volume: rho=0.564, p=0.001; manually delineated volume: rho=0.576, p=0.001).

[figure 6]

Remote Autobiographical Memory

Remote autobiographical memory scores correlated across patients with their reduced average thalamic (r=0.552, p-corr=0.009) and HPC GM volume (r=0.486, p-corr=0.036; left: r=0.486, p-unc=0.006; right: r=0.418, p-unc=0.019; table S3). Thalamic and HPC GM volumes correlated across patients (r=0.496, p=0.002). The effects of HPC atrophy on remote autobiographical memory were fully mediated by thalamic GM volume reduction (figure 7).

At uncorrected levels, manually delineated HPC volumes also correlated with these scores (total HPC: r=0.412, p-unc=0.021; Table S4). As total HPC volume correlated across patients with average thalamic GM volume (r=0.438, p=0.006), a mediation analysis was conducted, which disclosed full mediation of the effects of HPC atrophy on remote autobiographical memory by thalamic volume reduction (direct effect: β=0.505, p=0.210; indirect effect: β=0.453, 95% CI: 0.071, 0.881).

[figure 7]

Table 4 below summarizes the relationships identified between memory impairment and structural and functional abnormalities in patients, as related to the effects of HPC atrophy.

[table 4]

Discussion

We examined the brain abnormalities underlying episodic memory impairment in autoimmune LE, a clinical syndrome in which acute, focal inflammation in the HPC leads, in the long-term, to HPC atrophy and amnesia. We hypothesized that focal HPC damage would be accompanied by remote effects on the structure and function of the extended HPC system (Aggleton et al., 2010), and that these abnormalities would be instrumental in explaining patients' anterograde and retrograde amnesia.

Consistent with previous investigations in smaller cohorts (Butler et al., 2014; Finke et al., 2017; Henson et al., 2016; Irani et al., 2013; Malter et al., 2014), our patients showed selective deficits in episodic memory, in the face of normal levels of visuomotor, language, executive function, general and personal semantic memory. Episodic memory impairment was evident across a broad range of tests that have been extensively used in studies of MTL amnesia (Bayley et al., 2003; Vann et al., 2009). In terms of anterograde memory, patients showed impaired visual and verbal recall and recognition memory, and pronounced forgetting of visual material. Examining retrograde amnesia, we found striking loss of remote autobiographical memories from childhood and early adulthood.

The focal HPC high T2 signal on clinical MRI from the acute disease phase was followed by focal HPC atrophy within the MTL. However, patients also showed volume reduction in specific midline and lateral thalamic regions, along with reduced rsALFF in the PCC and precuneus, and reduced rsFC between the right HPC and the left HPC, the medial

prefrontal and posteromedial cortices - regions known to interact closely with the HPC in the healthy brain.

These abnormalities fully mediated the effects of HPC atrophy on memory performance. The only direct effect of HPC atrophy we observed was on forgetting, and no other brain abnormalities showed such an effect. Our results highlight the need to take into account the remote changes in brain structure and function that may be associated with focal HPC damage (Aggleton, 2014), since these may explain specific aspects of anterograde and retrograde amnesia and help identify others that may be a direct function of HPC atrophy per se.

Abnormalities in the extended HPC system following HPC atrophy

We found focal HPC atrophy using the gold standard of manual volumetry for MTL structures (Grimm et al., 2015). Automated segmentation of other subcortical structures disclosed no atrophy at group level. However, our uniquely large cohort enabled us to examine subtle structural abnormalities across the whole brain in a voxel-wise fashion.

Notably, volume reduction was observed, not only in the HPC, but also in anterior, dorsomedial, and dorsolateral thalamic regions, the nuclei within which are known to interact with the HPC and cingulate cortices (Aggleton et al., 2010). Our cross-sectional design cannot conclusively show that these extra-HPC abnormalities occurred as a consequence of focal HPC damage, and our findings should guide future longitudinal studies. Nevertheless, inflammatory pathology appeared confined to the HPC in the vast

majority of our patients, and would be expected to spread to adjacent areas, rather than to remote regions in the extended HPC network such as the thalamus or PCC. Post-mortem studies demonstrating focal HPC pathology in autoimmune LE patients (Khan et al., 2009; Park et al., 2007) and animal models (Tröscher et al., 2017) indicate that these regions are likely affected as a secondary consequence of HPC damage, rather than due to the primary pathology. Furthermore, the possibility of extra-HPC damage is equally if not more likely in other conditions associated with HPC amnesia, such as cases of ischemia/anoxia (Huang and Castillo, 2008). It should, however, be noted that a single case study of amnesia due to ischemia/anoxia which came to post mortem demonstrated focal neuronal loss in the CA1 region of the HPC on histopathology (Zola-Morgan et al., 1986). Direct comparisons between LE and amnesia due to different etiologies would be useful in future research.

Patients also showed functional abnormalities in the posteromedial cortex, and the effect of HPC atrophy on PCC rsALFF was fully mediated by the correlative volume reduction in the thalamic regions. This is consistent with the functional abnormalities previously observed in posteromedial cortical regions in both HPC and diencephalic amnesias in humans (Aggleton, 2014; Reed et al., 1999).

Patients also showed reduced inter-HPC rsFC. The spontaneous activity of the HPC is coupled with that of the contralateral HPC at rest and such connectivity is part of the default-mode network. This is also the case for the medial prefrontal and posteromedial cortical regions which showed reduced rsFC with the HPC (Buckner et al., 2008; Greicius et al., 2004). The decrease in inter-HPC rsFC across patients as a function of

delay since symptom onset is consistent with the idea that these network-wide abnormalities follow focal HPC damage. In future, this needs replication in longitudinal studies.

Anterograde Memory: Recall and recognition memory

Patients showed impairment across all tests of visual and verbal recall and recognition memory. The only unimpaired form of memory was face recognition. This would be predicted by some material-specific accounts of recognition memory (Bird and Burgess, 2008) and is consistent with the view that recognition of unfamiliar faces is exceptional in several regards, e.g. faces are holistically processed and difficult to label verbally, and adequate performance levels may be attained in the absence of capacities to associate faces with a study list (Smith et al., 2014). Ours is the largest study to date to confirm preserved face recognition memory in HPC amnesia.

At uncorrected levels, HPC volumes correlated with both recall and recognition memory scores. Crucially, however, the effects of HPC atrophy on verbal and visual recall and visual recognition were fully mediated by the correlative reduction in PCC rsALFF. This finding demonstrates that the HPC role in recall and recollection cannot be examined in isolation from remote effects of HPC damage within the extended HPC system. It furthermore dovetails with the causal role that has been attributed to the posteromedial cortex in episodic memory for both visual (Bonnì et al., 2015) and verbal (Koch et al., 2018) material, and aligns with evidence from neurodegenerative diseases that it is posteromedial cortex rather than hippocampal function that predicts episodic memory impairment (La Joie et al., 2014). Patients' impaired verbal recognition was associated

with reduced inter-HPC rsFC. The reasons why the correlates of verbal recognition were different from those of other forms of memory are unclear, but the relationship with inter-HPC rsFC is consistent with that found between inter-HPC connectivity and episodic memory in healthy (Wang et al., 2010) and patient populations (e.g. traumatic axonal injury) (Marquez de la Plata et al., 2011).

It should be noted that our neuropsychological assessment did not explicitly attempt to distinguish between the recollection and familiarity processes that may underlie differences in recall and recognition memory. In order to identify the neural mechanisms supporting these processes, finer-grained behavioral paradigms are required. Furthermore, our study did not include HPC subfield volumetry, which may have disclosed stronger correlations between HPC subfields and memory scores. The volumes and hemodynamic activity of HPC subfields have been associated with various forms of memory (Bonnici et al., 2013; Miller et al., 2017; Palombo et al., 2018). While imaging at higher field strength is required to investigate HPC subfields, our study highlights the fact that the remote effects of HPC damage on wider brain networks are a key factor in HPC amnesia.

Anterograde Memory: Forgetting

The only aspect of amnesia upon which HPC atrophy showed a direct effect was that of visual forgetting (of abstract shapes). Patients showed only a marginal increase in verbal forgetting, perhaps explained by the fact that HPC atrophy was less pronounced in the left than the right hemisphere. This is consistent with evidence for HPC lateralization of maintenance processes for verbal (left HPC) (Frisk and Milner, 1990)

and visual material (right HPC) (Smith and Milner, 1989). Indeed, rapid forgetting of visual information in right HPC damage was noted quite early (Jones-Gotman, 1986), as was, in general, the nature of forgetting in HPC amnesia (Huppert and Piercy, 1979). This has recently been re-emphasized (Sadeh et al., 2014), with functional neuroimaging studies in healthy young adults attributing a central role to the HPC in constraining the forgetting that occurs by new learning (Kuhl et al., 2010).

Our results go beyond these studies and demonstrate an exclusive relationship between HPC atrophy and rapid forgetting even within the context of abnormalities in the extended HPC system. This relationship is consistent with computational models of HPC function that outline pattern completion and pattern separation (O'Reilly and McClelland, 1994) as two core mechanisms that protect against forgetting. Pattern completion enables the reinstatement of previously encoded memories from incomplete input, whereas pattern separation involves the orthogonal coding of memories for overlapping events, which minimizes forgetting by generating non-interfering representations (Kuhl et al., 2010).

These findings suggest that the HPC role in amnesia may be much less direct than has previously been held, at least with respect to performance on widely used, standardized neuropsychological tests of memory. In contrast with the majority of such tests, the measurements of forgetting such as that used here partially control for factors that may confound simple recall scores, such as variability in attention, initial learning or retrieval strategy, factors that may depend on regions outside the HPC. Instead, measurements of forgetting may provide the most sensitive and specific way to detect

HPC damage. This proposal does not preclude the possibility that the HPC mechanisms underlying the retention of newly formed memories are process- or material-specific. As our forgetting rates were derived only from a recall-based test (Baddeley et al., 1994), we are unable to comment on the relationship of HPC atrophy with forgetting in recognition memory, a relationship which has recently been questioned (Sadeh et al., 2014). Likewise, material-specificity in rapid forgetting should be examined with finer-grained behavioral tasks, involving different types of stimuli (e.g. scenes vs. faces). Nevertheless, the direct relationship of (right) HPC atrophy with (visual) forgetting highlights the utility of tests of accelerated forgetting in detecting HPC pathology in other disorders. Recent studies have emphasized a possible role for such tests in the early detection of Alzheimer's disease pathology (Weston et al., 2018; Zimmermann and Butler, 2018).

Remote autobiographical memory

Patients showed spared remote personal semantic memory, in the face of impaired remote autobiographical memories. To date, research in autoimmune LE patients has focused on anterograde memory (Butler et al., 2014; Finke et al., 2017; Henson et al., 2016; Malter et al., 2014; Miller et al., 2017), with very little evidence on retrograde amnesia (Chan et al., 2007). Our study is also one of the very few to examine the relationship of focal HPC damage with both anterograde and retrograde amnesia.

It is possible that the test we used to assess remote memories (AMI) is insufficiently sensitive to truly 'episodic' aspects of autobiographical memory that have been held to be HPC-dependent (Moscovitch et al., 2016; Nadel and Moscovitch, 1997). Other

methods, involving parametric text-based procedures, may offer greater sensitivity [e.g. the Autobiographical Interview (Levine et al., 2002)]. Nevertheless, studies on other amnesic cohorts have found the AMI and the Autobiographical Interview to offer comparable results (Rensen et al., 2017).

Our findings would at first sight appear to support a role for the HPC in the recollection of remote autobiographical memories. Nevertheless, the effects of HPC atrophy were fully mediated by the GM volume reduction in the thalamus. Furthermore, no selective relationship was found between remote autobiographical memory scores and anterior or posterior HPC volumes. These findings are difficult to reconcile with the multiple trace (Moscovitch et al., 2005) or trace-transformation accounts of retrograde amnesia (Sekeres et al., 2018), according to which such deficits would be a function of the extent of HPC damage, either *in toto*, or in specific HPC portions.

The absence of direct effects of HPC atrophy on remote memory, in combination with the selective presence of such effects on forgetting rates, is instead consistent with the idea that HPC circuitry acts as a buffer for the temporary maintenance of episodic information, with non-HPC structures storing more permanent memory traces. Our findings may thus offer some support for the standard consolidation model of remote memory. Other work supporting this model has primarily emphasized the role of neocortical damage in retrograde amnesia (Bayley et al., 2003; Squire et al., 2015). We here highlight the need also to consider the role of the thalamus. Focal thalamic damage has been often associated with retrograde amnesia in single-case or small case-series studies (Carlesimo et al., 2011; Stuss et al., 1988), and mediodorsal thalamic nuclei may

coordinate the recollection of cortically stored memories (Miller et al., 2001) via thalamic-prefrontal cortical projections (Kopelman, 2015). Our results show that secondary alterations in thalamic integrity may explain the large variability in retrograde memory loss reported after HPC damage (Bartsch et al., 2011; Bayley et al., 2003; St-Laurent et al., 2011).

Conclusion

Our study, probably the largest in human HPC amnesia, shows that abnormalities in the integrity of and connectivity within the extended HPC system may occur after focal HPC damage, and that these play a central role in explaining the variability in the anterograde and retrograde amnesia of patients with HPC atrophy. We found that the neuropsychological measure most sensitive and specific to HPC atrophy was the forgetting of newly learned information. Understanding the impact of network-wide changes following HPC damage will be key to resolving long-standing controversies in the literature on human amnesia.

Materials and Methods

Participants

Patients

Inclusion and exclusion criteria

We identified 38 patients (26M:12F; age at research MRI: M=63.06; IQR=16.16 years; table 5) who i) had undergone neuropsychological assessment during the acute phase of the illness at the Russell Cairns Unit, Oxford (2013-2018); ii) had been diagnosed with LE according to the diagnostic criteria described in (Graus et al., 2016): a) subacute onset of memory deficits [1], seizures, or psychiatric symptoms suggesting involvement of the limbic system; b) bilateral brain abnormalities on T2-weighted MRI, restricted within the MTL; c) CSF pleocytosis (white blood cells >5/mm^3) and / or EEG with epileptic or slow-wave activity involving the temporal lobes; d) reasonable exclusion of alternative causes (e.g. CNS infections, septic encephalopathy, metabolic encephalopathy, drug toxicity, cerebrovascular disease, neoplastic disorders, Creutzfeldt-Jakob disease, epileptic disorders, rheumatologic disorders, Kleine-Levin, mitochondrial diseases); e) detection of antibodies against cell-surface, synaptic, or onconeural proteins. According to (Graus et al., 2016), criteria (a-d) are required for a diagnosis of 'definite LE', unless, in the absence of one of (a-c), criterion (e) is satisfied.

34/38 patients met the criteria for a diagnosis of 'definite LE'. The remaining 4 patients had been diagnosed with autoimmune LE, and satisfied criteria (a), (b), and (d), but not

[1] (Graus et al., 2016) mention 'working memory deficits'. However, other studies have used 'short-term memory' as a criterion [e.g. (Graus et al., 2004)] and the classical deficit is generally held to be in episodic memory [e.g. (Vincent et al., 2004)].

(e), and no data could be recovered on (c). In the majority of patients (28/38), an autoantibody known to be associated with LE had been identified, but 10/38 had the typical clinical profile of LE with no identified antibody. Such cases are well-recognised (Graus et al., 2018) and are likely here due to antibodies not detectable in routine clinical practice at the time of screening. No patient presented with NMDAR-antibody encephalitis (Malter et al., 2013) or positive polymerase chain reaction testing for herpes simplex virus. Only two cases (28,31) had identifiable neoplastic lesions that were treated and were in full remission at the time of study participation. 31/38 patients had been treated with immunotherapy (e.g. intravenous and/or oral prednisolone, plasma exchange) in the acute phase of the illness.

Furthermore, all patients i) had undergone MRI at the time of initial clinical presentation; ii) were fluent in English (37 native speakers; 1 non-native speaker); iii) had no history of previous psychiatric or neurological disorder that could have resulted in cognitive impairment and iv) had no contraindication to MRI at the time of entry into the study.

Patients were all recruited in the post-acute phase of the illness (M=5.41; IQR=5.36 years since symptom onset) and were re-assessed by an experienced neurologist (CRB) prior to study inclusion.

Acute Clinical MRI

Neuroradiological reports of patients' MRI scans from the time of initial clinical presentation were consulted to identify abnormalities in T2 signal, volume, and diffusion, within and beyond the MTL. 34/38 patients showed abnormal signal, volume (swelling or atrophy) and/or (facilitated) diffusion in the HPC. High signal in the amygdala was noted in 6/38 patients. One patient showed abnormalities in the entorhinal cortex, and one patient in the parahippocampal cortex (Table 5). No acute abnormalities were detected in 4/38 patients who nonetheless had clinical features characteristic of autoimmune LE. Only one patient showed extra-MTL abnormalities (bright caudate), and four patients had mild microangiopathic changes, which are commonly found with aging.

[table 5]

Healthy Controls

Healthy controls were recruited through local advertisement and through the Oxford Project To Investigate Memory and Aging. All were fluent in English (40 Native speakers; 1 non-native speaker).

All participants provided written informed consent according to the Declaration of Helsinki. Ethical approval was received from South Central Oxford Research Ethics Committee (REC no: 08/H0606/133).

Neuropsychological Assessment

All 38 patients (26M:12F; age at assessment: M=61.32; IQR=15.82 years) were assessed with neuropsychological tests, along with 41 control participants (27M:14F; age at assessment: M=61.50; IQR=16.93 years; controls vs. patients: age: U=706, p=0.477; M:F ratio: χ^2=0.059, p=0.808).

Neuropsychological tests were administered to assess the following domains: premorbid intelligence [National Adult Reading Test (NART) (Nelson and Willison, 1991)]; executive function [Wechsler Memory Scale III (WMS-III) digit span (Wechsler, 1997); Delis-Kaplan Executive Function System (DKEFS) Trails (Delis et al., 2001)]; semantic memory and language [Camel and Cactus Test (C&CT) (Bozeat et al., 2000); Graded Naming Test (GNT) (Mckenna and Warrington, 1980); Weschler Abbreviate Scale of Intelligence (WASI/WASI-II) Vocabulary and Similarity (Wechsler, 2011)]; visuospatial and motor function [Rey-Osterrieth Complex Figure Test (ROCFT) copy (Rey, 1959); DKEFS trails visual scanning, motor speed (Delis et al., 2001); Visual Object and Space Perception (VOSP) cube analysis, dot counting, position discrimination (Warrington and James, 1991)]; anxiety and depression [Hospital Anxiety and Depression Scale (HADS) (Zigmond and Snaith, 1983)].

Anterograde memory

Anterograde memory was examined using a range of memory tests: WMS-III (Wechsler, 1997); ROCFT (Rey, 1959); the Warrington Recognition Memory Tests for faces and

words (Warrington, 1984) and the Warrington Topographical Memory test for scenes (RMT) (Warrington, 1996); the Doors and People test (D&P) (Baddeley et al., 1994)].

Retrograde memory

In order to assess patients' remote autobiographical memory, we administered the most commonly used clinical test of autobiographical memory, the Autobiographical Memory Interview [AMI; (Kopelman et al., 1989)]. The AMI assesses semantic autobiographical memory ('personal semantics') through a structured interview concerning autobiographical facts. Episodic autobiographical memory is examined through the free recall of events and is scored (0-3) for specificity and richness of episodic recall. Following the AMI manual, 3 points were given for episodic memories produced in a highly detailed fashion, with mention of specific time and place; 0-2 points were given to memories recalled with poor episodic detail, i.e. 2 points were credited when the episodic memory was not recalled in detail or did not involve mention of time and place, or where the memory was not recalled; 1 point was given for a vague personal memory; and 0 points when a response was not provided or when general semantic information was provided instead (Kopelman et al., 1989). Memories of three periods are assessed: childhood (up to 18 years of age), early adulthood (up to participants' mid 30's), and recent memories (0-5 years from the time of the interview). We identified 31 patients (23M:8F; age at assessment: M=63.79, IQR=15.16 years) and 29 controls who were over the age of 50 at the time of assessment (19M:10F; age: M=65.74, IQR=17.23; controls vs. patients: age: U=431.00, p=0.789; M:F ratio: χ^2=0.537, p=0.464). As such, recent memories did not overlap with those of early adulthood (recent autobiographical / semantic memories probed by this test pertain to 0-5 years before the time of

assessment), and involved a minimum of 10 years between the earliest recent memory and the latest memory for early adulthood that the AMI probed.

Scores in the 'recent memory' conditions, which cover a period of 0-5 years preceding the date of assessment, at least partly reflected anterograde memory impairment, as they overlapped with the period post-disease onset (time since acute presentation (mean=5.99; SD=4.00 years). Indeed, of the 31 patients analyzed, only 1 reported recent memories formed premorbidly. The recent memory scores of the AMI could thus not capture retrograde amnesia for recent personal semantic and autobiographical memories, and were not considered in the analysis.

For the purposes of data reduction, minimization of measurement error, maximization of generalizability of our findings, and simplification of correlational analyses, we used i) anterograde memory composite scores for visual or verbal (immediate or delayed) recall or (immediate) recognition, by averaging the age-scaled, standardized scores of each patient across the tests of anterograde memory in which patients showed impairment; ii) a remote autobiographical memory score, by summing patients' AMI scores for autobiographical memories in childhood and early adulthood; iii) the D&P scores for verbal or visual forgetting - unlike other tests of immediate and delayed recall memory that involve no mechanism for equating participants on immediate recall, the D&P quantifies forgetting on the basis of participants' performance in the last trial of immediate recall relative to their performance in delayed recall.

Significant correlations between structural / functional abnormalities and any of the aforementioned composite scores were followed up by a series of correlations with: i) (immediate and delayed) verbal recall memory (WMS-III Logical Memory I, Word List I, D&P People) , ii) (immediate and delayed) visual recall memory (D&P Shapes, ROCFT Immediate Recall), iii) (immediate) verbal recognition memory (RMT Words, D&P Names), iv) (immediate) visual recognition memory (RMT Scenes, D&P Doors), v) verbal and vi) visual forgetting, vii) remote autobiographical memory.

Brain Imaging

Scanning procedures

Image acquisition was conducted on a Siemens 3T Trio system using a 32-channel head coil (University of Oxford Centre for Clinical Magnetic Resonance Research).

Structural MRI

3D T1-weighted images were acquired using a Magnetization Prepared Rapid Gradient Echo (MPRAGE) sequence (echo time=4.7ms, repetition time=2040ms, 8° flip angle, field of view=192mm, voxel size=1 x 1 x 1mm). All 38 patients (26M:12F; age at imaging: M=63.06; IQR=16.06 years) underwent structural brain imaging, along with all 67/67 control participants (35 recruited by the Memory and Amnesia Project; 32 datasets were made available through the Oxford Project To Investigate Memory and Aging; 40M:27F; age at imaging: M=64.70; IQR=19.87 years; controls vs. patients: M:F ratio: χ^2=0.79, p=0.374; age at imaging: U=1239.5, p=0.825).

Resting-state fMRI

BOLD-weighted fMRI data were acquired using a Gradient Echo EPI sequence. Participants were instructed to lay still, keep their eyes open to watch the fixation cross presented on the in-scanner projector, and not to fall asleep. Whole-brain data were acquired (180 volumes; slice thickness=3.5mm, echo time=28ms, repetition time=2410ms, 89° flip angle, field of view=192mm, voxel size=3 x 3 x 3.5mm). 35/38 patients (3 datasets were discarded due to acquisition errors and/or movement; 24M:11F; age at imaging: M=61.45; IQR=15.85 years) underwent resting-state fMRI, along with 32/67 control participants (3 datasets discarded due to acquisition errors and/or movement; only structural MRIs were available for the remaining 32 controls that were made available through the Oxford Project To Investigate Memory and Aging; 23M:9F; median=55.71; IQR=17.18 years; controls vs. patients: M:F ratio: χ^2=0.087, p=0.768; age at imaging: U=425.00, p=0.091).

GM volume, hemodynamic activity, and functional connectivity

Volumetry

Manual segmentation of MTL

Manual segmentation of the MTL (38/38 patients; 48/67 healthy controls) was carried out in native space using ITK-SNAP (Yushkevich et al., 2006) by a trained researcher (ARF) (protocol: https://www.ndcn.ox.ac.uk/files/research/segmentation_protocol_medial_temporal_lobes.pdf). Segmentation procedures were based on published atlases and protocols (Insausti et al., 1998; Pruessner et al., 2002). The structures delineated were the HPC, amygdala, and the perirhinal, entorhinal, parahippocampal, and temporopolar cortices.

Structures were segmented in each hemisphere. Intra-rater reliability was measured using intra-class coefficient correlations on a random selection of 24 hemispheres (12 patients and 12 controls) segmented twice by ARF with an interval of at least 4 months between segmentations. Intra-rater reliability matched that reported for manual MTL segmentations (Olsen et al., 2013) (HPC: 0.98; amygdala: 0.80; perirhinal cortex: 0.90; entorhinal cortex: 0.82; parahippocampal cortex: 0.93; temporopolar cortex: 0.96;).

The volumes of all structures were corrected for total intra-cranial volume (TIV) derived from the unified segmentation procedure in SPM12 (see below) and expressed as z scores based on the mean volume and SD of individually age-matched controls for each patient (+/- 10 years; number of controls per patient: M=23; IQR=11).

Automated segmentation of other subcortical structures

The brainstem, thalamus, caudate nucleus, putamen, and pallidum were also automatically segmented using FSL FIRST (v. 6.0 http://www.fmrib.ox.ac.uk/fsl) (Patenaude et al., 2011) for all participants. Volumes were corrected for TIV and expressed as z scores as above..

Voxel-based morphometry

To identify GM volume discrepancies between groups at a whole-brain level, the T1-weighted images were analysed with VBM (Ashburner and Friston, 2000), using the Statistical Parametric Mapping software (SPM12 v7219; http://www.fil.ion.ucl.ac.uk/spm/software/spm12) running in Matlab R2017b.

Images were examined for scanner artefacts, reoriented to have the same point of origin (anterior commissure) and spatial orientation, bias-corrected to remove intensity non-uniformities, and segmented into GM, white matter (WM), and cerebrospinal fluid (CSF), using the unified segmentation procedure (Ashburner and Friston, 2005). The diffeomorphic anatomical registration through the exponentiated lie algebra (DARTEL) toolbox was applied to all participants' GM, WM, and CSF to refine inter-subject registration, and study-specific GM templates were generated (Ashburner, 2007). After affine registration of the GM DARTEL templates to the tissue probability maps in MNI (Montreal Neurological Institute, Quebec, Canada) space, non-linear warping of GM images was performed to the DARTEL GM template in MNI space. Voxel values in the tissue maps were modulated by the Jacobian determinant (calculated during spatial normalization), with modulated GM images reflecting tissue volume. These images (voxel size: 1 mm^3 isotropic) were smoothed using a standard Gaussian filter (4 mm FWHM) to increase spatial specificity within MTL structures. We compared GM volume between groups, including age, sex, and TIV as second-level covariates. We report clusters surviving FWE-correction ($p < .05$) at peak-voxel level over $p < .001$ (uncorrected).

The mean GM volumes of VBM clusters were extracted using the Marsbar toolbox in SPM12 (Brett et al., 2002), were residualized across participants against age, sex, and TIV, and were used in a series of bivariate correlations with memory scores across patients.

fMRI analysis

Resting-state fMRI preprocessing and connectivity analyses were conducted using the CONN toolbox version 18.a (https://www.nitrc.org/projects/conn) (Whitfield-Gabrieli and Nieto-Castanon, 2012) in SPM.

Preprocessing

The EPIs were spatially realigned to correct for interscan movement and were slice time-corrected. The structural MRIs were coregistered to the EPIs, segmented and normalized along with EPIs in MNI space, followed by motion outlier detection (ART-based scrubbing). Denoising including the anatomical component-based correction method (CompCor) (Behzadi et al., 2007) was used to remove sources of noise in the BOLD time series data, deriving principal components from WM and CSF. WM, CSF and the six movement parameters were included as first-level nuisance covariates. A temporal band pass filter (0.01-0.1 Hz) was applied to this residual BOLD signal to remove motion artefacts, physiological and other artefactual effects. Images were smoothed using a Gaussian filter (8 mm FWHM).

We explored resting-state functional abnormalities in patients with respect to both segregation and integration, i.e. in terms of hemodynamic activity in local regions, or in functional connectivity between regions. We used data-driven approaches in both.

Resting-state Hemodynamic Activity: rsALFF

We examined local abnormalities in the intensity of slow spontaneous fluctuations of hemodynamic activity at rest across the whole brain, using an analysis of amplitude of low-frequency fluctuations (rsALFF) (Zang et al., 2007). RsALFF is defined as the total power within the low-frequency range (0.01-0.1 Hz), and thus indexes the strength or intensity of low frequency oscillations; rsALFF has been linked to neuronal glucose metabolism (Tomasi et al., 2013) and correlates with local field potential activity (Logothetis et al., 2001). Alterations in rsALFF have been shown in a number of disorders (Küblböck et al., 2014; Kwak et al., 2012; Lui et al., 2015), and can also reflect individual differences in performance in a large variety of cognitive tasks (Mennes et al., 2011; Wei et al., 2012). We opted for ALFF over fALFF (fractional amplitude of low frequency fluctuations, i.e. the total power within the low-frequency range, divided by the total power in the entire detectable frequency range), as the former demonstrates higher test–retest reliability in GM regions, which suggests that it is potentially more sensitive for discerning differences between individuals and groups (Zuo et al., 2010).

Resting-state Functional Connectivity: Multivariate Pattern Analysis

In order to identify seed regions for post-hoc seed-to-voxel connectivity analyses in a data-driven fashion, we used multivariate pattern analysis (MVPA) as implemented in the connectome-MVPA CONN toolbox (Whitfield-Gabrieli and Nieto-Castanon, 2012). MVPA assesses the multivariate pattern of pairwise connections between voxels across the whole brain by performing a principal component analysis separately for each voxel that characterizes its rsFC with the rest of the brain. In the first step,

separately for each subject, a default number of 64 principal components were retained while characterizing each subject's voxel-to-voxel correlation structure. The resulting component scores were stored as first-level voxel-to-voxel covariance matrices for each subject. In the second step, jointly across subjects and separately for each voxel, the 7 strongest components were retained from a principal component decomposition of the between-subjects variability in seed-to-voxel connectivity maps between this voxel and the rest of the brain, in keeping with a conventionally used conservative 1:10 ratio between the number of components extracted and the number of subjects (n=67). Second-level analyses were then performed to test for group differences in whole-brain connectivity by means of an F-test across all MVPA components, comparing for each voxel the component scores across the two groups (covariates: age, sex). The results for each voxel reflected between-group rsFC differences between this voxel and the rest of the brain.

Resting-state FC: Seed-to-voxel connectivity analysis

The MVPA was followed up by post-hoc analyses to determine specific connectivity patterns in the data. We therefore conducted a whole-brain seed-to-voxel rsFC analysis, seeding from the regions identified from the MVPA contrast (controls vs. patients; covariates: age, sex), to explore connectivity between those regions and the rest of the brain.

All three resting-state fMRI analyses described above involved an F contrast (controls < > patients; covariates: age, sex), with statistical parametrical connectivity maps

thresholded at a voxel level of $p < 0.001$ and FWE-corrected ($p < .05$) at cluster- or voxel peak-level.

Relationships among structural and functional abnormalities

Given our hypothesis that focal HPC atrophy is associated with abnormalities in interconnected areas of a broader network, we explored the relationships between volume reduction and functional abnormalities across patients, using a series of bivariate correlations and mediation analyses, with HPC volumes as the independent variable, other structural abnormalities as the mediator variables, and functional abnormalities as the dependent variables (see below).

Relationship with delay from symptom onset

Given our hypothesis that broader network abnormalities occur after focal HPC atrophy, we also assessed the relationship of the delay between symptom onset and research participation with the extent of HPC and extra-HPC structural and functional abnormalities in a series of bivariate correlations.

Structure/Function-Behavior Correlations

Given our *a priori* hypothesis regarding the relationship of HPC atrophy with both memory impairment and abnormalities in the extended HPC system, correlations of HPC volumes (average GM of VBM clusters or manually delineated volumes) with memory scores and extra-HPC structural (average GM of VBM clusters) or functional abnormalities (mean rsFC and rsALFF of clusters) were investigated at uncorrected

levels (p-unc < 0.05; see below). Correlations of extra-HPC abnormalities with memory scores were corrected for multiple testing (see below).

We examined the relationship of each abnormality with patients' verbal or visual recognition, verbal or visual recall composite scores, their overall remote autobiographical memory scores [AMI (Kopelman et al., 1989)], and their visual or verbal forgetting scores from the Doors and People test (Baddeley et al., 1994).

Given our hypothesis that HPC atrophy gives rise to a series of correlative abnormalities in regions within broader networks that may themselves be associated with memory impairment, we conducted a series of mediation analyses (see below): HPC volumes were entered as the independent variables, and memory scores as the dependent variables. Mediator variables were structural or functional abnormalities that were correlated with both HPC volumes and memory scores across patients.

Measures of structural or functional abnormality that did not correlate with each other across patients but were both associated with impaired memory scores were entered as independent variables in a series of multiple step-wise linear regression analyses (dependent variable: memory scores), in order to investigate the portion of the variance of memory impairment that could be explained by each of those abnormalities (see below).

Experimental Design and Statistical Analysis

Non-imaging statistical analyses were performed using SPSS (version 25.0, SPSS Inc). Variance homogeneity was assessed using Levene's test, and normal distribution using the Shapiro-Wilk test. Parametric (Student t-test; Welch t-test used when the assumption of homogeneity of variances was violated) and non-parametric tests (Mann-Whitney U employed when the assumption of normal distribution was not met in a group) were used appropriately. Pearson correlation coefficient (r) and Spearman's rho (ρ) (when variables were not normally distributed) were used to examine the relationship among measures of structural, functional abnormality, and memory scores. Significance values were corrected ('p-corr') for multiple comparisons and correlations with the Holm-Bonferroni sequential correction method (Holm, 1979), unless otherwise stated ('p-unc'), as in the case of correlations between HPC volumes and memory scores. In cases where correction for multiple comparisons does not apply, 'p' was used instead.

Mediation analyses

Mediation is a hypothesis about a causal relation among variables (Judd & Kenny, 1981, Baron & Kenny, 1986, MacKinnon et al., 2007). Four conditions are required to be met to establish mediation: i) the independent variable must be associated with the dependent variable; ii) the independent variable must be associated with the mediator; iii) the mediator variable must be associated with the dependent variable; iv) the mediator variable mediates the relationship between the independent and the dependent variable if controlling for the mediator variable reduces the variance of the dependent variable explained by the independent variable.

Mediation models were computed utilizing PROCESS v. 3.0 (Hayes, 2012). Since the product of the two variables is normally distributed only in large samples, we used bootstrapping (5000 samples) to construct bias-corrected and accelerated 95% confidence intervals (CIs) around a point estimate of the indirect effect (Mackinnon et al., 2004; Preacher and Hayes, 2008). This procedure tested the null hypothesis that the indirect path from the interaction term to the dependent variable via the mediator does not differ from 0. If 0 is not contained within the CIs computed by the bootstrapping procedure, the indirect effect is inferred to differ from 0 at $p < 0.05$.

Multiple step-wise linear regression analyses

We assessed the proportion of the variance of memory scores that was explained by structural and functional abnormalities across patients by entering measures of such abnormalities (that were not significantly correlated across patients) in a series of multiple step-wise linear regression analyses as independent variables (default alpha level of 0.05 for entry to model and 0.1 for removal).

Acknowledgments

We are very grateful to the participants who took part in this study, as well as to Prof. Andy Lee (University of Toronto Scarborough) for his helpful feedback on an earlier version of this manuscript, and to Prof. Ricardo Insausti (University of Castilla-La Mancha) for his advice regarding manual segmentations.

SRI is supported by the Wellcome Trust (104079/Z/14/Z), the UCB-Oxford University Alliance, BMA Research Grants- Vera Down grant (2013) and Margaret Temple (2017), Epilepsy Research UK (P1201) and by the Fulbright UK-US commission (MS-SOCIETY research AWARD). The research was funded /supported by the National Institute for Health Research (NIHR) Oxford Biomedical Research Centre (BRC; The views expressed are those of the author(s) and not necessarily those of the NHS, the NIHR or the Department of Health).

CRB is supported by a Medical Research Council Clinician Scientist Fellowship (MR/K010395/1).

1 **Competing Interests**

2 SRI is a coapplicant and receives royalties on patent application WO/2010/046716
3 (U.K. patent no., PCT/GB2009/051441) entitled 'Neurological Autoimmune Disorders'.
4 The patent has been licensed to Euroimmun AG for the development of assays for LGI1
5 and other VGKC-complex antibodies. The other authors declare no competing financial
6 interests.

References

Addis DR, Moscovitch M, McAndrews MP. 2007. Consequences of hippocampal damage across the autobiographical memory network in left temporal lobe epilepsy. *Brain* **130**:2327–2342. doi:10.1093/brain/awm166

Aggleton JP. 2014. Looking beyond the hippocampus: old and new neurological targets for understanding memory disorders. *Proc R Soc B Biol Sci* **281**:20140565–20140565. doi:10.1098/rspb.2014.0565

Aggleton JP, O'Mara SM, Vann SD, Wright NF, Tsanov M, Erichsen JT. 2010. Hippocampal-anterior thalamic pathways for memory: uncovering a network of direct and indirect actions. *Eur J Neurosci* **31**:2292–2307. doi:10.1111/j.1460-9568.2010.07251.x

Ashburner J. 2007. A fast diffeomorphic image registration algorithm. *Neuroimage* **38**:95–113.

Ashburner J, Friston KJ. 2005. Unified segmentation. *Neuroimage* **26**:839–51. doi:10.1016/j.neuroimage.2005.02.018

Ashburner J, Friston KJ. 2000. Voxel-Based Morphometry—the methods. *Neuroimage* **11**:805–821. doi:10.1006/nimg.2000.0582

Baddeley A, Emslie H, Nimmo-Smith I. 1994. Doors and people: a test of visual and verbal recall and recognition. Bury St. Edmunds, England: Thames Valley Test Co.

Bartsch T, Döhring J, Rohr A, Jansen O, Deuschl G. 2011. CA1 neurons in the human hippocampus are critical for autobiographical memory, mental time travel, and autonoetic consciousness. *Proc Natl Acad Sci U S A* **108**:17562–7. doi:10.1073/pnas.1110266108

30 Bayley PJ, Hopkins RO, Squire LR. 2003. Successful Recollection of Remote
31 Autobiographical Memories by Amnesic Patients with Medial Temporal Lobe
32 Lesions. *Neuron* **38**:135–144. doi:10.1016/S0896-6273(03)00156-9

33 Behzadi Y, Restom K, Liau J, Liu TT. 2007. A component based noise correction method
34 (CompCor) for BOLD and perfusion based fMRI. *Neuroimage* **37**:90–101.
35 doi:10.1016/J.NEUROIMAGE.2007.04.042

36 Bird CM, Burgess N. 2008. The hippocampus supports recognition memory for familiar
37 words but not unfamiliar faces. *Curr Biol* **18**:1932–1936.
38 doi:10.1016/j.cub.2008.10.046

39 Bonnì S, Veniero D, Mastropasqua C, Ponzo V, Caltagirone C, Bozzali M, Koch G. 2015.
40 TMS evidence for a selective role of the precuneus in source memory retrieval.
41 *Behav Brain Res* **282**:70–75. doi:10.1016/J.BBR.2014.12.032

42 Bonnici HM, Chadwick MJ, Maguire EA. 2013. Representations of recent and remote
43 autobiographical memories in hippocampal subfields. *Hippocampus* **23**:849–54.
44 doi:10.1002/hipo.22155

45 Bozeat S, Lambon Ralph MA, Patterson K, Garrard P, Hodges JR. 2000. Non-verbal
46 semantic impairment in semantic dementia. *Neuropsychologia* **38**:1207–1215.
47 doi:10.1016/S0028-3932(00)00034-8

48 Brett M, Anton J-L, Valabregue R, Poline J-B. 2002. Region of interest analysis using an
49 SPM toolbox [abstract]8th International Conference on Functional Mapping of the
50 Human Brain.

51 Brown MW, Aggleton JP. 2001. Recognition memory: What are the roles of the
52 perirhinal cortex and hippocampus? *Nat Rev Neurosci* **2**:51–61.

53 doi:10.1038/35049064

54 Buckner RL, Andrews-Hanna JR, Schacter DL. 2008. The brain's default network:
55 Anatomy, function, and relevance to disease. *Ann N Y Acad Sci* **1124**:1–38.
56 doi:10.1196/annals.1440.011

57 Butler CR, Miller TD, Kaur MS, Baker IW, Boothroyd GD, Illman NA, Rosenthal CR,
58 Vincent A, Buckley CJ. 2014. Persistent anterograde amnesia following limbic
59 encephalitis associated with antibodies to the voltage-gated potassium channel
60 complex. *J Neurol Neurosurg Psychiatry* **85**:387–91. doi:10.1136/jnnp-2013-
61 306724

62 Carlesimo GA, Lombardi MG, Caltagirone C. 2011. Vascular thalamic amnesia: A
63 reappraisal. *Neuropsychologia* **49**:777–789.
64 doi:10.1016/J.NEUROPSYCHOLOGIA.2011.01.026

65 Carter AR, Astafiev S V., Lang CE, Connor LT, Rengachary J, Strube MJ, Pope DLW,
66 Shulman GL, Corbetta M. 2009. Resting state inter-hemispheric fMRI connectivity
67 predicts performance after stroke. *Ann Neurol* **67**:NA-NA. doi:10.1002/ana.21905

68 Chan D, Henley SMD, Rossor MN, Warrington EK. 2007. Extensive and temporally
69 ungraded retrograde amnesia in encephalitis associated with antibodies to voltage-
70 gated potassium channels. *Arch Neurol* **64**:404–410.
71 doi:10.1001/archneur.64.3.404

72 Damasio AR, Van Hoesen GW. 1985. The limbic system and the localisation of herpes
73 simplex encephalitis. *J Neurol Neurosurg Psychiatry* **48**:297–301.
74 doi:10.1136/jnnp.48.4.297

75 Delis DCD, Kaplan E, Kramer JH, Delis DC, Kaplan E, Kramer JH. 2001. Delis-Kaplan

executive function system (D-KEFS), Canadian Journal of School Psychology. Psychological Corporation.

Finke C, Prüss H, Heine J, Reuter S, Kopp UA, Wegner F, Bergh FT, Koch S, Jansen O, Münte T, Deuschl G, Ruprecht K, Stöcker W, Klaus-Peterwandinger KP, Paul F, Bartsch T. 2017. Evaluation of cognitive deficits and structural hippocampal damage in encephalitis with leucine-rich, glioma-inactivated 1 antibodies. *JAMA Neurol* **74**:50–59. doi:10.1001/jamaneurol.2016.4226

Frisk V, Milner B. 1990. The role of the left hippocampal region in the acquisition and retention of story content. *Neuropsychologia* **28**:349–359. doi:10.1016/0028-3932(90)90061-R

Gitelman DR, Ashburner J, Friston KJ, Tyler LK, Price CJ. 2001. Voxel-based morphometry of herpes simplex encephalitis. *Neuroimage* **13**:623–631. doi:10.1006/nimg.2000.0734

Graham KS, Barense MD, Lee ACHH. 2010. Going beyond LTM in the MTL: a synthesis of neuropsychological and neuroimaging findings on the role of the medial temporal lobe in memory and perception. *Neuropsychologia* **48**:831–53. doi:10.1016/j.neuropsychologia.2010.01.001

Graus F, Delattre JY, Antoine JC, Dalmau J, Giometto B, Grisold W, Honnorat J, Smitt PS, Yedeler C, Verschuuren JJGM, Vincent A, Voltz R. 2004. Recommended diagnostic criteria for paraneoplastic neurological syndromes. *J Neurol Neurosurg Psychiatry*. doi:10.1136/jnnp.2003.034447

Graus F, Escudero D, Oleaga L, Bruna J, Villarejo-Galende A, Ballabriga J, Barceló MI, Gilo F, Popkirov S, Stourac P, Dalmau J. 2018. Syndrome and outcome of antibody-negative limbic encephalitis. *Eur J Neurol* **25**:1011–1016. doi:10.1111/ene.13661

Graus F, Titulaer MJ, Balu R, Benseler S, Bien CG, Cellucci T, Cortese I, Dale RC, Gelfand JM, Geschwind M, Glaser CA, Honnorat J, Höftberger R, Iizuka T, Irani SR, Lancaster E, Leypoldt F, Prüss H, Rae-Grant A, Reindl M, Rosenfeld MR, Rostásy K, Saiz A, Venkatesan A, Vincent A, Wandinger K-P, Waters P, Dalmau J. 2016. A clinical approach to diagnosis of autoimmune encephalitis. *Lancet Neurol* **15**:391–404. doi:10.1016/S1474-4422(15)00401-9

Greicius MD, Srivastava G, Reiss AL, Menon V. 2004. Default-mode network activity distinguishes Alzheimer's disease from healthy aging: evidence from functional MRI. *Proc Natl Acad Sci U S A* **101**:4637–4642. doi:10.1073/pnas.0308627101

Grimm O, Pohlack S, Cacciaglia R, Winkelmann T, Plichta MM, Demirakca T, Flor H. 2015. Amygdalar and hippocampal volume: A comparison between manual segmentation, Freesurfer and VBM. *J Neurosci Methods* **253**:254–261. doi:10.1016/j.jneumeth.2015.05.024

Hardt O, Nadel L. 2018. Systems consolidation revisited, but not revised: The promise and limits of optogenetics in the study of memory. *Neurosci Lett* **680**:54–59. doi:10.1016/J.NEULET.2017.11.062

Hassabis D, Kumaran D, Vann SD, Maguire EA. 2007. Patients with hippocampal amnesia cannot imagine new experiences. *Proc Natl Acad Sci U S A* **104**:1726–31. doi:10.1073/pnas.0610561104

Hayes AF. 2012. PROCESS: A versatile computational tool for observed variable mediation, moderation, and conditional process modeling [White paper].

Hayes SM, Salat DH, Verfaellie M. 2012. Default network connectivity in medial temporal lobe amnesia. *J Neurosci* **32**:14622–14629a. doi:10.1523/JNEUROSCI.0700-12.2012

124 Henson RN, Greve A, Cooper E, Gregori M, Simons JS, Geerligs L, Erzinçlioğlu S, Kapur N,
125 Browne G, Geerligs L, Erzinc S. 2016. The effects of hippocampal lesions on MRI
126 measures of structural and functional connectivity. *Hippocampus* **26**:1447–1463.
127 doi:10.1002/hipo.22621

128 Henson RN, Horner AJ, Greve A, Cooper E, Gregori M, Simons JS, Erzinçlioğlu S, Browne
129 G, Kapur N. 2017. No effect of hippocampal lesions on stimulus-response bindings.
130 *Neuropsychologia* **103**:106–114. doi:10.1016/j.neuropsychologia.2017.07.024

131 Holm S. 1979. A simple sequentially rejective multiple test procedure. *Scand J Stat* **6**:65–
132 70. doi:10.2307/4615733

133 Huang BY, Castillo M. 2008. Hypoxic-ischemic brain injury: imaging findings from birth
134 to adulthood. *RadioGraphics* **28**:417–439. doi:10.1148/rg.282075066

135 Huppert FA, Piercy M. 1979. Normal and Abnormal Forgetting in Organic Amnesia:
136 Effect of Locus of Lesion. *Cortex* **15**:385–390. doi:10.1016/S0010-9452(79)80065-
137 9

138 Insausti R, Juottonen K, Soininen H, Insausti AM, Partanen K, Vainio P, Laakso MP,
139 Pitkänen A. 1998. MR volumetric analysis of the human entorhinal, perirhinal, and
140 temporopolar cortices. *Am J Neuroradiol* **19**:659–671.

141 Irani SR, Michell AW, Lang B, Pettingill P, Waters P, Johnson MR, Schott JM, Armstrong
142 RJE, S. Zagami A, Bleasel A, Somerville ER, Smith SMJ, Vincent A. 2011.
143 Faciobrachial dystonic seizures precede Lgi1 antibody limbic encephalitis. *Ann*
144 *Neurol* **69**:892–900. doi:10.1002/ana.22307

145 Irani SR, Stagg CJ, Schott JM, Rosenthal CR, Schneider SA, Pettingill P, Pettingill R, Waters
146 P, Thomas A, Voets NL, Cardoso MJ, Cash DM, Manning EN, Lang B, Smith SJM,

147 Vincent A, Johnson MR. 2013. Faciobrachial dystonic seizures: The influence of
148 immunotherapy on seizure control and prevention of cognitive impairment in a
149 broadening phenotype. *Brain* **136**:3151–3162. doi:10.1093/brain/awt212

150 Jones-Gotman M. 1986. Right hippocampal excision impairs learning and recall of a list
151 of abstract designs. *Neuropsychologia* **24**:659–670. doi:10.1016/0028-
152 3932(86)90005-9

153 Kafkas A, Migo EM, Morris RG, Kopelman MD, Montaldi D, Mayes AR. 2016. Material
154 specificity drives medial temporal lobe familiarity but not hippocampal
155 recollection. *Hippocampus* **209**:1–20. doi:10.1002/hipo.22683

156 Khan NL, Jeffree MA, Good C, Macleod W, Al-Sarraj S. 2009. Histopathology of VGKC
157 antibody-associated limbic encephalitis. *Neurology* **72**:1703–5.
158 doi:10.1212/WNL.0b013e3181a55eb3

159 Kim S, Dede AJO, Hopkins RO, Squire LR. 2015. Memory, scene construction, and the
160 human hippocampus. *Proc Natl Acad Sci U S A* **112**:4767–72.
161 doi:10.1073/pnas.1503863112

162 Koch G, Bonnì S, Pellicciari MC, Casula EP, Mancini M, Esposito R, Ponzo V, Picazio S, Di
163 Lorenzo F, Serra L, Motta C, Maiella M, Marra C, Cercignani M, Martorana A,
164 Caltagirone C, Bozzali M. 2018. Transcranial magnetic stimulation of the precuneus
165 enhances memory and neural activity in prodromal Alzheimer's disease.
166 *Neuroimage* **169**:302–311. doi:10.1016/J.NEUROIMAGE.2017.12.048

167 Kopelman MD. 2015. What does a comparison of the alcoholic Korsakoff syndrome and
168 thalamic infarction tell us about thalamic amnesia? *Neurosci Biobehav Rev* **54**:46–
169 56. doi:10.1016/J.NEUBIOREV.2014.08.014

170 Kopelman MD, Wilson BA, Baddeley AD. 1989. The autobiographical memory interview:
171 a new assessment of autobiographical and personal semantic memory in amnesic
172 patients. *J Clin Exp Neuropsychol* **11**:724–744. doi:10.1080/01688638908400928

173 Kotsenas AL, Watson RE, Pittock SJ, Britton JW, Hoye SL, Quek AML, Shin C, Klein CJ.
174 2014. MRI findings in autoimmune voltage-gated potassium channel complex
175 encephalitis with seizures: One potential etiology for mesial temporal sclerosis. *Am*
176 *J Neuroradiol*. doi:10.3174/ajnr.A3633

177 Küblböck M, Woletz M, Höflich A, Sladky R, Kranz GS, Hoffmann A, Lanzenberger R,
178 Windischberger C. 2014. Stability of low-frequency fluctuation amplitudes in
179 prolonged resting-state fMRI. *Neuroimage* **103**:249–257.
180 doi:10.1016/J.NEUROIMAGE.2014.09.038

181 Kuhl BA, Shah AT, DuBrow S, Wagner AD. 2010. Resistance to forgetting associated with
182 hippocampus-mediated reactivation during new learning. *Nat Neurosci* **13**:501–
183 506. doi:10.1038/nn.2498

184 Kwak Y, Peltier SJ, Bohnen NI, Müller MLTM, Dayalu P, Seidler RD. 2012. L-DOPA
185 changes spontaneous low-frequency BOLD signal oscillations in Parkinson's
186 disease: a resting state fMRI study. *Front Syst Neurosci* **6**:52.
187 doi:10.3389/fnsys.2012.00052

188 La Joie R, Landeau B, Perrotin A, Bejanin A, Egret S, Pélerin A, Mézenge F, Belliard S, de
189 La Sayette V, Eustache F, Desgranges B, Chételat G. 2014. Intrinsic Connectivity
190 Identifies the Hippocampus as a Main Crossroad between Alzheimer's and
191 Semantic Dementia-Targeted Networks. *Neuron* **81**:1417–1428.
192 doi:10.1016/J.NEURON.2014.01.026

193 Lambon Ralph MA, Moriarty L, Sage K, Ackerman T, Arul K, Bird H, Crisp J, Davies S, Ellis

194 A, Harold R, Heaney P, Jones M, Knapp S, Luff H, McKinnon R, Morris J, Newton A,
195 Raynor R, Sharpe S, Southwell L, Swinson J, Taylor L, Walker E, Whitton E, Ralph
196 MAL, Moriarty L, Sage K. 2002. Anomia is simply a reflection of semantic and
197 phonological impairments: Evidence from a case-series study. *Aphasiology* **16**:56–
198 82. doi:10.1080/02687040143000448

199 Lambon Ralph MA, Patterson K, Plaut DC. 2011. Finite case series or infinite single-case
200 studies? Comments on "Case series investigations in cognitive neuropsychology" by
201 Schwartz and Dell (2010). *Cogn Neuropsychol* **28**:466–474.
202 doi:10.1080/02643294.2012.671765

203 Logothetis NK, Pauls J, Augath M, Trinath T, Oeltermann A. 2001. Neurophysiological
204 investigation of the basis of the fMRI signal. *Nature* **412**:150–157.
205 doi:10.1038/35084005

206 Lui S, Yao L, Xiao Y, Keedy SK, Reilly JL, Keefe RS, Tamminga CA, Keshavan MS, Pearlson
207 GD, Gong Q, Sweeney JA. 2015. Resting-state brain function in schizophrenia and
208 psychotic bipolar probands and their first-degree relatives. *Psychol Med* **45**:97–
209 108. doi:10.1017/S003329171400110X

210 Mackinnon DP, Lockwood CM, Williams J. 2004. Confidence limits for the indirect effect:
211 distribution of the product and resampling methods. *Multivariate Behav Res* **39**:99.
212 doi:10.1207/s15327906mbr3901_4

213 Maguire EA, Mullally SL. 2013. The hippocampus: a manifesto for change. *J Exp Psychol*
214 *Gen* **142**:1180–9. doi:10.1037/a0033650

215 Maguire EA, Nannery R, Spiers HJ. 2006. Navigation around London by a taxi driver with
216 bilateral hippocampal lesions. *Brain* **129**:2894–2907. doi:10.1093/brain/awl286

217 Malter MP, Elger CE, Surges R. 2013. Diagnostic value of CSF findings in antibody-
218 associated limbic and anti-NMDAR-encephalitis. *Seizure* **22**:136–140.
219 doi:10.1016/J.SEIZURE.2012.12.013

220 Malter MP, Frisch C, Schoene-Bake JC, Helmstaedter C, Wandinger KP, Stoecker W,
221 Urbach H, Surges R, Elger CE, Vincent A V., Bien CG. 2014. Outcome of limbic
222 encephalitis with VGKC-complex antibodies: relation to antigenic specificity. *J*
223 *Neurol* **261**:1695–1705. doi:10.1007/s00415-014-7408-6

224 Marquez de la Plata CD, Garces J, Shokri Kojori E, Grinnan J, Krishnan K, Pidikiti R,
225 Spence J, Devous MD, Moore C, McColl R, Madden C, Diaz-Arrastia R. 2011. Deficits
226 in functional connectivity of hippocampal and frontal lobe circuits after traumatic
227 axonal injury. *Arch Neurol* **68**:74–84. doi:10.1001/archneurol.2010.342

228 Mckenna P, Warrington EK. 1980. Testing for nominal dysphasia. *J Neurol Neurosurgery,*
229 *Psychiatry* **43**:781–788. doi:10.1136/jnnp.43.9.781

230 Mennes M, Zuo X-N, Kelly C, Di Martino A, Zang Y-F, Biswal B, Castellanos FX, Milham
231 MP. 2011. Linking inter-individual differences in neural activation and behavior to
232 intrinsic brain dynamics. *Neuroimage* **54**:2950–2959.
233 doi:10.1016/J.NEUROIMAGE.2010.10.046

234 Miller LA, Caine D, Harding A, Thompson EJ, Large M, Watson JD. 2001. Right medial
235 thalamic lesion causes isolated retrograde amnesia. *Neuropsychologia* **39**:1037–
236 1046. doi:10.1016/S0028-3932(01)00041-0

237 Miller TD, Chong TT-J, Aimola Davies AM, Ng TWC, Johnson MR, Irani SR, Vincent A,
238 Husain M, Jacob S, Maddison P, Kennard C, Gowland PA, Rosenthal CR. 2017. Focal
239 CA3 hippocampal subfield atrophy following LGI1 VGKC-complex antibody limbic
240 encephalitis. *Brain* **140**:1212–1219. doi:10.1093/brain/awx070

241 Moscovitch M, Cabeza R, Winocur G, Nadel L. 2016. Episodic Memory and Beyond: The
242 Hippocampus and Neocortex in Transformation. *Annu Rev Psychol* **67**.
243 doi:10.1146/annurev-psych-113011-143733

244 Moscovitch M, Rosenbaum RS, Gilboa A, Addis DR, Westmacott R, Grady C, McAndrews
245 MP, Levine B, Black S, Winocur G, Nadel L. 2005. Functional neuroanatomy of
246 remote episodic, semantic and spatial memory: a unified account based on multiple
247 trace theory. *J Anat* **207**:35–66. doi:10.1111/j.1469-7580.2005.00421.x

248 Nadel L, Moscovitch M. 1997. Memory consolidation, retrograde amnesia and the
249 hippocampal complex. *Curr Opin Neurobiol* **7**:217–27.

250 Nelson HE, Willison J. 1991. National Adult Reading Test (NART): Test manual.

251 O'Reilly RC, McClelland JL. 1994. Hippocampal conjunctive encoding, storage, and recall:
252 Avoiding a trade-off. *Hippocampus* **4**:661–682. doi:10.1002/hipo.450040605

253 Olsen RK, Palombo DJ, Rabin JS, Levine B, Ryan JD, Rosenbaum RS. 2013. Volumetric
254 analysis of medial temporal lobe subregions in developmental amnesia using high-
255 resolution magnetic resonance imaging. *Hippocampus* **23**:855–860.
256 doi:10.1002/hipo.22153

257 Palombo DJ, Bacopulos A, Amaral RSC, Olsen RK, Todd RM, Anderson AK, Levine B.
258 2018. Episodic autobiographical memory is associated with variation in the size of
259 hippocampal subregions. *Hippocampus* **28**:69–75. doi:10.1002/hipo.22818

260 Park DC, Murman DL, Perry KD, Bruch LA. 2007. An autopsy case of limbic encephalitis
261 with voltage-gated potassium channel antibodies. *Eur J Neurol* **14**:e5–e6.
262 doi:10.1111/j.1468-1331.2007.01924.x

263 Patenaude B, Smith SM, Kennedy DN, Jenkinson M. 2011. A Bayesian model of shape and

264 appearance for subcortical brain segmentation. *Neuroimage* **56**:907–922.
265 doi:10.1016/j.neuroimage.2011.02.046

266 Preacher KJ, Hayes AF. 2008. Asymptotic and resampling strategies for assessing and
267 comparing indirect effects in multiple mediator models. *Behav Res Methods*
268 **40**:879–891. doi:10.3758/BRM.40.3.879

269 Pruessner JC, Köhler S, Crane J, Pruessner M, Lord C, Byrne A, Kabani N, Collins DL,
270 Evans AC. 2002. Volumetry of temporopolar, perirhinal, entorhinal and
271 parahippocampal cortex from high-resolution MR images: considering the
272 variability of the collateral sulcus. *Cereb Cortex* **12**:1342–1353.
273 doi:10.1093/cercor/12.12.1342

274 Reed LJ, Marsden P, Lasserson D, Sheldon N, Lewis P, Stanhope N, Guinan E, Kopelman
275 MD. 1999. FDG-PET Analysis and Findings in Amnesia Resulting From Hypoxia.
276 *Memory* **7**:599–614. doi:10.1080/096582199387779

277 Rensen YCM, Kessels RPC, Migo EM, Wester AJ, Eling PATM, Kopelman MD. 2017.
278 Personal semantic and episodic autobiographical memories in Korsakoff
279 syndrome: A comparison of interview methods. *J Clin Exp Neuropsychol* **39**:534–
280 546. doi:10.1080/13803395.2016.1248811

281 Rey A. 1959. Manuel du test de copie d'une figure complexe de A. Rey. *Paris Les Ed du*
282 *Cent Psychol Appliquée*.

283 Rudebeck SR, Filippini N, Lee ACH. 2013. Can complex visual discrimination deficits in
284 amnesia be attributed to the medial temporal lobe? An investigation into the effects
285 of medial temporal lobe damage on brain connectivity. *Hippocampus* **23**:7–13.
286 doi:10.1002/hipo.22056

Sadeh T, Ozubko JD, Winocur G, Moscovitch M. 2014. How we forget may depend on how we remember. *Trends Cogn Sci* **18**:26–36. doi:10.1016/J.TICS.2013.10.008

Scoville WB, Milner B. 1957. Loss of recentmemory after bilateral hippocampal lesions. *J Neurol Neurosurg Psychiatry* **20**:11–21. doi:10.1136/jnnp.20.1.11

Sekeres MJ, Winocur G, Moscovitch M. 2018. The hippocampus and related neocortical structures in memory transformation. *Neurosci Lett* **680**:39–53. doi:10.1016/J.NEULET.2018.05.006

Smith CN, Jeneson A, Frascino JC, Kirwan CB, Hopkins RO, Squire LR. 2014. When recognition memory is independent of hippocampal function. *Proc Natl Acad Sci U S A* **111**:9935–40. doi:10.1073/pnas.1409878111

Smith M Lou, Milner B. 1989. Right hippocampal impairment in the recall of spatial location: Encoding deficit or rapid forgetting? *Neuropsychologia* **27**:71–81. doi:10.1016/0028-3932(89)90091-2

Squire LR, Genzel L, Wixted JT, Morris RG. 2015. Memory consolidation. *Cold Spring Harb Perspect Biol* **7**:a021766. doi:10.1101/cshperspect.a021766

Squire LR, Wixted JT. 2011. The cognitive neuroscience of human memory since H.M. *Annu Rev Neurosci* **34**:259–88. doi:10.1146/annurev-neuro-061010-113720

Squire LR, Zola SM. 1996. Ischemic brain damage and memory impairment: a commentary. *Hippocampus* **6**:546–52. doi:10.1002/(SICI)1098-1063(1996)6:5<546::AID-HIPO7>3.0.CO;2-G

St-Laurent M, Moscovitch M, Tau M, McAndrews MP. 2011. The temporal unraveling of autobiographical memory narratives in patients with temporal lobe epilepsy or excisions. *Hippocampus* **21**:409–421. doi:10.1002/hipo.20757

310 Stuss DT, Guberman A, Nelson R, Larochelle S. 1988. The neuropsychology of
311 paramedian thalamic infarction. *Brain Cogn* **8**:348–378. doi:10.1016/0278-
312 2626(88)90059-0

313 Thompson J, Bi M, Murchison AG, Makuch M, Bien CG, Chu K, Farooque P, Gelfand JM,
314 Geschwind MD, Hirsch LJ, Somerville E, Lang B, Vincent A, Leite MI, Waters P, Irani
315 SR, Dogan-Onugoren M, Rae-Grant A, Illes Z, Szots M, Malter M, Widman G, Surges
316 R, Archibald N, Reid J, Duncan C, Richardson A, Lilleker J, Iorio R, Blaabjerg M,
317 Abeler K, Shin Y. 2018. The importance of early immunotherapy in patients with
318 faciobrachial dystonic seizures. *Brain* **141**:348–356. doi:10.1093/brain/awx323

319 Tomasi D, Wang G-J, Volkow ND. 2013. Energetic cost of brain functional connectivity.
320 *Proc Natl Acad Sci U S A* **110**:13642–7. doi:10.1073/pnas.1303346110

321 Tröscher AR, Klang A, French M, Quemada-Garrido L, Kneissl SM, Bien CG, Pákozdy Á,
322 Bauer J. 2017. Selective limbic blood–brain barrier breakdown in a feline model of
323 limbic encephalitis with LGI1 antibodies. *Front Immunol* **8**:1364.
324 doi:10.3389/fimmu.2017.01364

325 Vann SD, Tsivilis D, Denby CE, Quamme JR, Yonelinas AP, Aggleton JP, Montaldi D, Mayes
326 AR. 2009. Impaired recollection but spared familiarity in patients with extended
327 hippocampal system damage revealed by 3 convergent methods. *Proc Natl Acad Sci*
328 *U S A* **106**:5442–7. doi:10.1073/pnas.0812097106

329 Veldsman M, Curwood E, Pathak S, Werden E, Brodtmann A. 2018. Default mode
330 network neurodegeneration reveals the remote effects of ischaemic stroke. *J Neurol*
331 *Neurosurg Psychiatry* **89**:318–320. doi:10.1136/jnnp-2017-315676

332 Vincent A, Buckley C, Schott JM, Baker I, Dewar BK, Detert N, Clover L, Parkinson A, Bien
333 CG, Omer S, Lang B, Rossor MN, Palace J. 2004. Potassium channel antibody-

associated encephalopathy: A potentially immunotherapy-responsive form of limbic encephalitis. *Brain* **127**:701–712. doi:10.1093/brain/awh077

Wang L, Negreira A, LaViolette P, Bakkour A, Sperling RA, Dickerson BC. 2010. Intrinsic interhemispheric hippocampal functional connectivity predicts individual differences in memory performance ability. *Hippocampus* **20**:345–351. doi:10.1002/hipo.20771

Warrington E. 1984. The Recognition Memory Test. Windsor, UK: NFER-Nelson.

Warrington EK. 1996. The Camden Memory Tests. Psychology Press.

Warrington EK, James M. 1991. The Visual Object and Space Perception Battery, Thames Valley Test Company.

Wechsler D. 2011. WASI -II: Wechsler abbreviated scale of intelligence - second edition, WASI. Psychological Corporation.

Wechsler D. 1997. Wechsler Memory Scale, Third. ed. San Antonio, TX: The Psychological Corporation.

Wei T, Liang X, He Y, Zang Y, Han Z, Caramazza A, Bi Y. 2012. Predicting conceptual processing capacity from spontaneous neuronal activity of the left middle temporal gyrus. *J Neurosci* **32**:481–9. doi:10.1523/JNEUROSCI.1953-11.2012

Weston PSJ, Nicholas JM, Henley SMD, Liang Y, Macpherson K, Donnachie E, Schott JM, Rossor MN, Crutch SJ, Butler CR, Zeman AZ, Fox NC. 2018. Accelerated long-term forgetting in presymptomatic autosomal dominant Alzheimer's disease: a cross-sectional study. *Lancet Neurol* **17**:123–132. doi:10.1016/S1474-4422(17)30434-9

Whitfield-Gabrieli S, Nieto-Castanon A. 2012. Conn: A functional connectivity toolbox for correlated and anticorrelated brain networks. *Brain Connect* **2**:125–141.

357 doi:10.1089/brain.2012.0073

358 Wixted JT, Squire LR. 2010. The role of the human hippocampus in familiarity-based
359 and recollection-based recognition memory. *Behav Brain Res* **215**:197–208.
360 doi:10.1016/j.bbr.2010.04.020

361 Yushkevich PA, Piven J, Hazlett HC, Smith RG, Ho S, Gee JC, Gerig G. 2006. User-guided
362 3D active contour segmentation of anatomical structures: Significantly improved
363 efficiency and reliability. *Neuroimage* **31**:1116–1128.
364 doi:10.1016/j.neuroimage.2006.01.015

365 Zang Y-F, He Y, Zhu C-Z, Cao Q-J, Sui M-Q, Liang M, Tian L-X, Jiang T-Z, Wang Y-F. 2007.
366 Altered baseline brain activity in children with ADHD revealed by resting-state
367 functional MRI. *Brain Dev* **29**:83–91. doi:10.1016/j.braindev.2006.07.002

368 Zigmond AS, Snaith RP. 1983. The Hospital Anxiety and Depression Scale. *Acta Psychiatr*
369 *Scand* **67**:361–370. doi:10.1111/j.1600-0447.1983.tb09716.x

370 Zimmermann JF, Butler CR. 2018. Accelerated long-term forgetting in asymptomatic
371 APOE ε4 carriers. *Lancet Neurol* **17**:394–395. doi:10.1016/S1474-4422(18)30078-
372 4

373 Zola-Morgan S, Squire LR, Amaral DG. 1986. Human amnesia and the medial temporal
374 region: enduring memory impairment following a bilateral lesion limited to field
375 CA1 of the hippocampus. *J Neurosci* **6**:2950–67.

376 Zuo X-N, Di Martino A, Kelly C, Shehzad ZE, Gee DG, Klein DF, Castellanos FX, Biswal BB,
377 Milham MP. 2010. The oscillating brain: Complex and reliable. *Neuroimage*
378 **49**:1432–1445. doi:10.1016/J.NEUROIMAGE.2009.09.037

379

Table 1: Neuropsychological profile of patients and healthy controls (post-acute phase)

Domain		Test	Subtest	controls		patients		Controls vs Patients			'Impaired' range		
				M	IQR	M	IQR	Test	Statistic	p-corr	cut-off score	Patients (n)	Controls (n)
Episodic Memory	Immediate Verbal Recall	WMS-III	Logical Memory I (z)	0.33	1.92	-1.00	1.34	t	6.78	< 0.0001	≤ - 1.67	14	0
			Word List I (z)	0.67	1.83	-1.00	1.51	U	178.00	< 0.0001	≤ - 1.67	11	0
		D&P	People (z)	-0.33	1.59	-1.33	1.00	U	266.00	< 0.0001	≤ - 1.67	15	1
	Delayed Verbal Recall	WMS-III	Logical Memory II (z)	0.67	1.67	-2.00	2.00	U	106.50	< 0.0001	≤ - 1.67	23	0
			Word List II (z)	1.33	1.00	-0.67	2.00	U	209.00	< 0.0001	≤ - 1.67	3	0
	Verbal Forgetting	D&P	Verbal Forgetting (z)	0.67	1.00	-0.33	1.75	U	415.50	0.1	≤ - 1.67	8	1
	Verbal Recognition		Names (z)	0.33	2.00	-1.00	2.00	t	5.16	< 0.0001	≤ - 1.67	13	1
		RMT	Words (z)	1.00	1.51	0.00	2.26	U	317.50	0.0002	≤ - 1.67	9	4
	Immediate Visual Recall	D&P	Shapes (z)	0.67	1.00	-0.84	2.08	Wt	6.06	< 0.0001	≤ - 1.67	13	0
		ROCFT	Immediate Recall (z)	1.26	1.93	-0.93	2.58	U	255.50	< 0.0001	≤ - 1.67	12	1
	Delayed Visual Recall		Delayed Recall (z)	1.26	1.98	-1.37	3.55	U	258.00	< 0.0001	≤ - 1.67	16	1
	Visual Forgetting	D&P	Visual Forgetting (z)	0.33	0.00	0.33	1.83	U	433.00	0.01	≤ - 1.67	8	1
	Visual Recognition		Doors (z)	0.67	1.33	-0.67	1.75	t	3.74	0.007	≤ - 1.67	7	1
		RMT	Scenes (z)	1.00	0.99	-0.35	2.65	U	281.00	0.003	≤ - 1.67	9	0
			Faces (z)	0.00	2.33	-0.33	1.66	t	1.29	0.7	≤ - 1.67	8	6
	Autobiographical Memory	AMI	Childhood (9)	9.00	3.00	4.50	4.00	U	153.50	0.0001	≤ 3 *	11	1
			Early Adulthood (9)	9.00	1.50	4.00	4.13	U	102.50	< 0.0001	≤ 3 *	14	0
Intelligence, Semantic Memory, and Language	Personal Semantic Memory		Childhood (21)	19.50	3.00	17.50	5.00	U	251.50	0.1	≤ 11 *	3	0
			Early Adulthood (21)	20.50	2.00	19.00	2.75	U	249.00	0.1	≤ 14 *	4	1
		NART	p-FSIQ (z)	1.44	0.85	1.07	1.30	U	485.00	0.1	≤ - 1.67	0	0
		WASI/	Vocabulary (z)	1.40	1.25	0.80	1.10	t	2.65	0.1	≤ - 1.67	0	0

		WASI-II	Similarities (z)	1.05	0.80	0.70	0.93	U	360.50	0.1	≤ - 1.67	0	0
		GNT	(z)	0.63	0.98	0.15	1.89	U	423.50	0.1	≤ - 1.67	5	0
		C&CT	(z)	0.34	1.22	0.02	1.22	U	496.50	0.1	≤ - 1.67	5	0
Executive Function		WMS-III	Digit Span (z)	0.84	1.25	0.33	1.67	t	2.70	0.1	≤ - 1.67	2	1
		DKEFS Trails	Number-Letter Switching (z)	0.67	0.67	0.33	1.00	U	470.00	0.1	≤ - 1.67	3	1
Visuomotor Function			Visual Scanning (z)	0.67	1.50	0.00	1.34	U	584.00	0.7	≤ - 1.67	5	4
			Motor Speed (z)	0.67	1.00	0.33	1.34	U	552.00	0.5	≤ - 1.67	7	5
		ROCFT	copy rank	> 16th %ile	0.00	> 16th %ile	0.00	U	619.00	0.5	≤ 16th %ile	2	1
		VOSP	Cube Analysis (z)	10.00	1.00	9.00	2.00	U	531.00	0.5	≤ 6 **	3	0
			Dot Counting (z)	10.00	0.00	10.00	0.00	U	625.50	0.7	≤ 8 **	1	1
			Position Discrimination (z)	20.00	0.00	20.00	1.00	U	631.00	0.7	≤ 18 **	4	2
Mood		HADS	Anxiety (21)	4.00	4.00	5.00	5.50	U	420.00	0.1	≥ 15	3	0
			Depression (21)	1.00	1.00	3.00	4.50	U	298.00	0.0006	≥ 15	0	0

AMI: Autobiographical Memory Interview; D&P: Doors and People Test; DKEFS: Delis-Kaplan Executive Function System; GNT: Graded Naming Test; HADS: Hospital Anxiety and Depression Scale; NART: National Adult Reading Test; RMT: Warrington Recognition Memory Tests (words, faces) and Warrington Topographical Memory test (scenes); ROCFT: Rey-Osterrieth Complex Figure Test; VOSP: Visual Object and Space Perception Battery; WASI/WASI-II Wechsler Abbreviated Scale of Intelligence; WMS-III: Wechsler Memory Scale III; *,**,***: no standardized scores available for these subtests; *: highest score of 'definitely abnormal' range, i.e. scores at or below which none of the healthy controls scored in (Kopelman et al., 1989); **: 5% cut-off score; ***: cut-off score for severe range; IQR: Inter-Quartile Range; M: median; *t*: Student's t-test; *U*: Mann-Whitney U; *Wt*: Welch's t-test; p-corr: p values are corrected using the Holm-Bonferroni sequential correction for multiple comparisons.

Table 2: Volumetry of MTL and subcortical structures in LE patients

Structure	Mean (z)	SD (z)	vs. z = -1 SD from age-matched healthy controls	
			t	p-corr
Hippocampus	-2.20	1.98	-3.73	0.0058
Entorhinal Cortex	-1.28	1.42	-1.21	0.5216
Perirhinal Cortex	-0.64	1.21	1.83	0.3789
Parahippocampal Cortex	-0.70	1.29	1.45	0.5216
Temporopolar Cortex	0.09	1.09	6.15	* < 0.0005
Amygdala	-0.36	2.06	1.92	0.3782
Thalamus	-0.75	1.02	1.52	0.5216
Brainstem	-0.06	1.04	5.56	* < 0.0005
Caudate Nucleus	-0.18	1.24	4.05	* 0.0025
Pallidum	-0.34	1.18	3.44	* 0.0116
Putamen	-0.48	1.10	2.91	* 0.0432
Nucleus Accumbens	-0.61	1.54	1.55	0.5216

Volumetry of manually and automatically delineated MTL and other subcortical structures of all patients (n = 38). Volumes for each structure are divided by TIV and expressed as z scores based on the mean and SD of the volumes of individually age-matched controls (+/- 10 years of age) for each patient. Hippocampal volumes were significantly lower than -1.5 SD (traditional cut-off point designating atrophy) from their age-matched controls' mean hippocampal volumes (t = -2.17, p = 0.037). A series of one-sample comparisons against a hypothesized mean of z = – 1 SD from the mean of controls' volumes were conducted to identify structures that showed milder atrophy in patients; no structure other than the hippocampus showed atrophy; *: volumes significantly above the atrophy threshold (but not enlarged). MTL: medial temporal lobe; p-corr: p values are adjusted with the Holm-Bonferroni sequential correction method for multiple comparisons; SD: standard deviation; t: one-sample t-test; TIV: total intracranial volume.

Table 3: GM volume reduction in patients (whole-brain VBM)

kE	Peak					center of mass			Structure
	p-FWE	t	x	y	z	x	y	z	
2262	< 0.0005	8.16	28	-17	-20	27	-15	-19	r anterior HPC (head extending to body)
1383	< 0.0005	7.21	-28	-14	-17	-26	-18	-18	l anterior HPC (head extending to body)
2009	< 0.0005	6.97	19	-28	6	10	-18	8	r anterior / mediodorsal / dorsolateral thalamic nuclei
605	< 0.0005	6.76	-2	-8	8	-4	-13	6	l anterior / mediodorsal thalamus
122	0.0046	5.78	-17	-23	9	-14	-23	9	l dorsolateral thalamus

Contrast: controls > patients; covariates: age, sex, TIV. Clusters are FWE-corrected at peak-voxel level ($p < .05$) over an individual voxel threshold of $p < .001$ (unc.); voxel size: 1 mm^3 isotropic; spatial smoothing kernel: 4 mm FWHM; FWHM: Full-width at half-maximum; HPC: hippocampus; kE: cluster size (number of voxels; minimum cluster size: 50 voxels); L: Left; mm: millimeter; R: Right (hemisphere).

Table 4: Summary of relationships between memory impairment and structural / functional abnormalities across patients

Memory Composite Score		**Effects of HPC atrophy**
Anterograde Memory	**Verbal Recognition**	Does not explain additional variance beyond that explained by inter-HPC rsFC reduction
	Visual Recognition	Fully mediated by PCC rsALFF reduction
	Verbal Recall	
	Visual Recall	
	Visual Forgetting	Direct effect - not mediated by extra-HPC abnormalities
Remote Autobiographical Memory		Fully mediated by thalamic GM volume reduction

GM: grey matter; HPC: hippocampus; PCC: posterior cingulate cortex; rsALFF: resting-state amplitude of low frequency fluctuations; rsFC: resting-state functional connectivity.

Table 5: Clinical details of LE patients (acute phase)

Code	Age (years)	Sex	Antibody Type	Acute T2 scan notes		
				HPC		Other structures
				R	L	
1	65.75	M	LGI1	Normal T2 signal and volume; facilitated diffusion	High T2 signal; swelling; normal diffusion	L AMG: high T2 signal
2	69.98	F	VGKCC	Normal T2 signal; mild atrophy; facilitated diffusion	High T2 signal; normal volume; facilitated diffusion	No abnormalities
3	62.23	M	VGKCC	Normal T2 signal and volume; facilitated diffusion	High T2 signal; swelling; normal diffusion	L AMG, L ERC: high T2 signal
4	46.41	M	LGI1	High T2 signal; normal volume; normal diffusion	Normal T2 signal and volume; facilitated diffusion	No abnormalities
5	56.65	M	LGI1	L/R: high T2 signal		No abnormalities
6	58.18	M	LGI1	No abnormalities		
7	56.13	M	LGI1	Normal volume and signal	High T2 signal; swelling	L/R AMG: high T2 signal
8	76.54	M	LGI1	High T2 signal; normal volume and diffusion	High T2 signal; normal volume; facilitated diffusion	No abnormalities
9	54.94	M	LGI1	High T2 signal; swelling; normal diffusion	High T2 signal; swelling; normal diffusion	No abnormalities
10	44.81	M	LGI1	L/R: high T2 signal; swelling		No abnormalities
11	45.77	M	LGI1	High T2 signal; normal volume	High T2 signal; normal volume	No abnormalities
12	46.06	M	LGI1/ Caspr2	High T2 signal; atrophy	Normal T2 signal and volume	No abnormalities
13	35.75	M	LGI1/ Caspr2	L/R: normal T2 signal; mild atrophy; normal diffusion		No abnormalities
14	72.08	M	LGI1	High T2 signal; mild atrophy; facilitated diffusion	Normal T2 signal; atrophy; facilitated diffusion	No abnormalities
15	52.28	M	LGI1	High T2 signal; normal volume; facilitated diffusion	Normal T2 signal and volume; facilitated diffusion	No abnormalities
16	52.48	M	LGI1/ Caspr2	High T2 signal; swelling; facilitated diffusion	Normal T2 signal and volume; facilitated diffusion	No abnormalities
17	51.62	M	VGKCC	High T2 signal; swelling	Normal T2 signal and volume	No abnormalities
18	75.18	M	LGI1	L/R: high T2 signal; swelling; normal diffusion		L/R AMG: high T2 signal; swelling
19	78.73	M	LG1/ Caspr2	High T2 signal; mild atrophy; normal diffusion	High T2 signal; normal volume; normal diffusion	No abnormalities
20	53.75	F	LGI1	L/R: high T2 signal; normal volume and diffusion		No abnormalities
21	73.68	F	VGKCC	L/R: high T2 signal; swelling; facilitated diffusion		No abnormalities

22	63.59	M	LGI1	L/R: high T2 signal; normal volume and diffusion	No abnormalities
23	60.35	M	VGKCC	No abnormalities	
24	54.30	M	VGKCC	L/R: high T2 signal; atrophy	L/R AMG: high T2 signal; atrophy
25	52.70	M	seronegative	L/R: high T2 signal	No abnormalities
26	47.43	F	seronegative	No abnormalities	
27	58.60	M	seronegative	L/R: high T2 signal	No abnormalities
28	25.42	M	Anti-Ma2	L/R: high T2 signal and swelling	No abnormalities
29	45.77	F	seronegative	L/R: high T2 signal	No abnormalities
30	16.64	F	GAD	No abnormalities	
31	71.35	M	seronegative	L/R: high T2 signal; atrophy	No abnormalities
32	60.44	M	VGKCC	L/R: atrophy	PHC atrophy
33	53.48	M	seronegative	L/R: atrophy	No abnormalities
34	64.87	F	seronegative	L/R: atrophy	No abnormalities
35	47.32	F	seronegative	L/R: high T2 signal	R AMG: high T2 signal; swelling
36	61.88	F	seronegative	L/R: high T2 signal; atrophy	No abnormalities
37	71.90	F	seronegative	L/R: high T2 signal (especially R)	No abnormalities
38	34.49	F	GAD	L/R: high T2 signal	No abnormalities

Age: age at symptom onset (years); M = male; F = female; Caspr2: anti-contactin-associated protein-like 2; GAD: anti-glutamic acid decarboxylase autoantibody; LGI1: anti-leucine-rich glioma-inactivated1; VGKCC: anti-voltage-gated potassium channel complex; AMG: Amygdala; ERC: entorhinal cortex; HPC: hippocampus; PHC: parahippocampal cortex; L, R: left, right hemisphere.

Figure 1: Reduction in GM volume, rsALFF and rsFC in LE

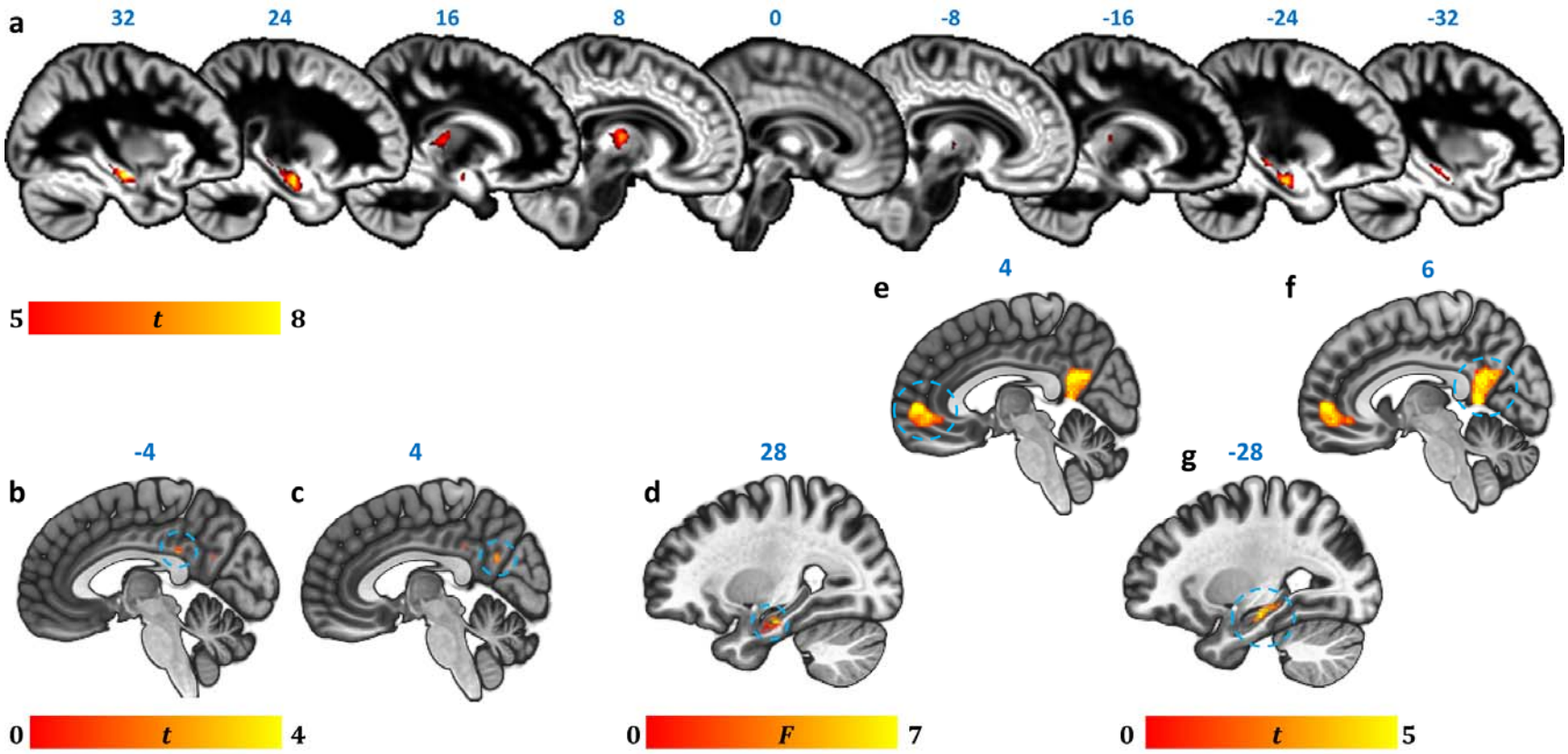

a: A whole-brain VBM on GM volume (contrast: controls > patients) showed bilateral volume reduction in patients' HPC and thalami (table 3); clusters survive FWE peak-level correction ($p < .05$) over $p < .001$ unc; color bar indicates t values; b-c: Reduced rsALFF in patients in (b) the posterior cingulate (kE = 89, p-FWE = 0.033; peak voxel coordinates: -4, -36, 28) and (c) precuneus (kE = 137; p-FWE = 0.003; peak voxel coordinates: 4, -60, 26); d-j: reduced rsFC in patients; d: a whole-brain MVPA (omnibus F) showed abnormal rsFC for patients in a cluster in the right HPC (kE = 178, p-FWE = 0.001; peak voxel coordinates: 28, -16,-20; color bar indicates F values); e-g: reduced rsFC of the right HPC (whole-brain seed-to-voxel analysis; seed: right HPC, anatomically delineated in native space, unsmoothed timeseries; contrast: controls > patients); e: medial prefrontal cortex (kE = 1152, p-FWE < 0.0001, peak voxel coordinates: 4, 56, 2); f: posteromedial cortex (posterior cingulate, retrosplenial cortex, precuneus; kE = 986, p-FWE < 0.0001, peak voxel coordinates: 6, -50, 8); g: left HPC (kE = 393, p-FWE < 0.0001, peak voxel coordinates: -12, -36, 2). All rsFC and rsALFF clusters survive FWE correction ($p < .05$) for cluster size over an individual voxel threshold of $p < .001$; FWE: family-wise error; HPC: hippocampus; kE: cluster size (number of voxels); rsALFF: Resting-state amplitude of low frequency fluctuations; rsFC: Resting-state functional connectivity; VBM: voxel-based morphometry.

Figure 2: Verbal Recognition Memory: Structural / Functional correlates

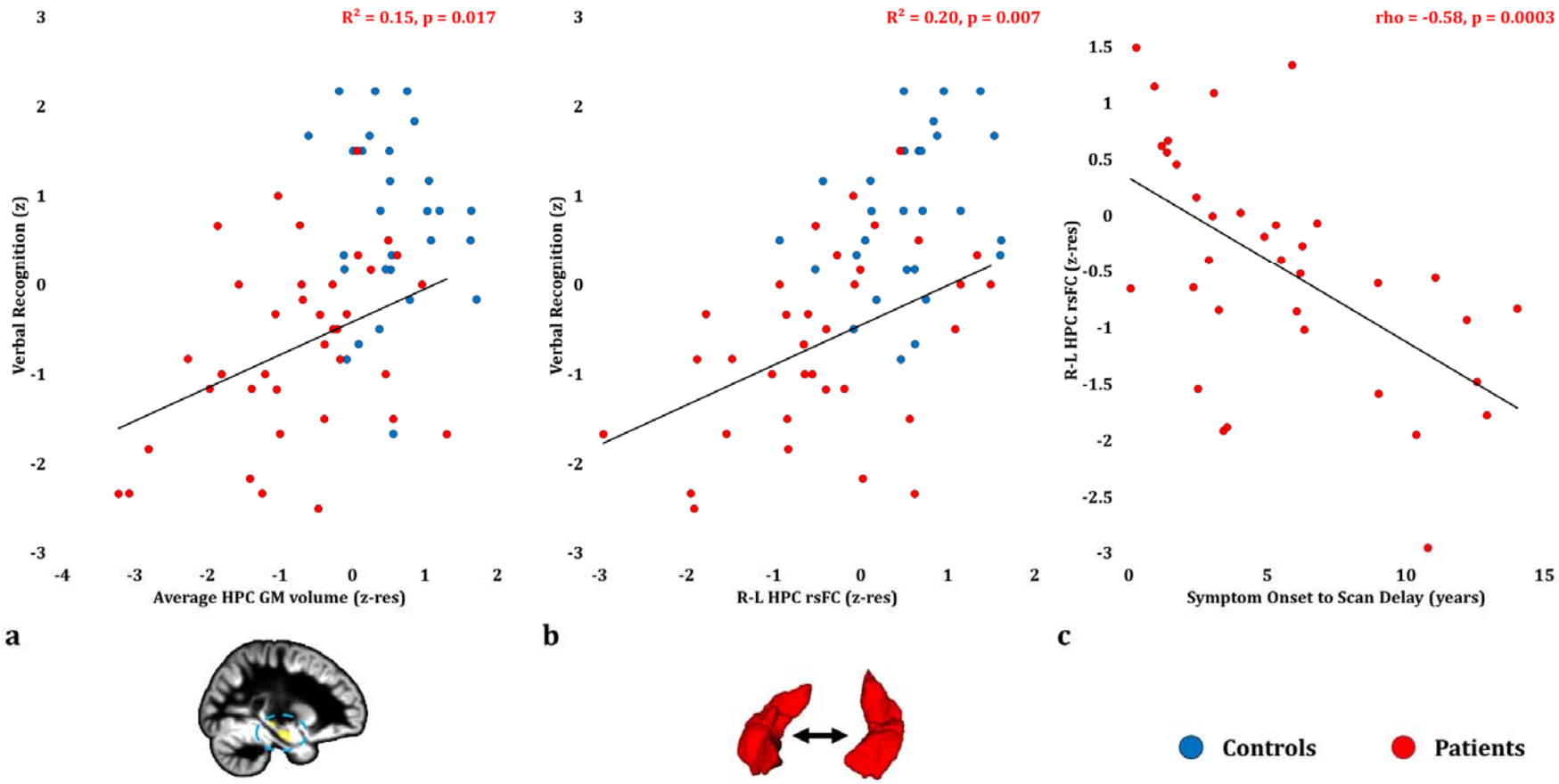

a: average GM volumes from the two HPC clusters (VBM) correlated across patients with their verbal recognition composite memory scores; b: mean inter-HPC rsFC correlated across patients with their verbal recognition composite memory scores; c: inter-HPC rsFC decreased across patients as a function of the delay between symptom onset and research scan; mean GM volume from VBM clusters is residualized against age, sex, and TIV across participants; mean rsFC is residualized across participants against age and sex; memory scores are averaged age-scaled and standardized scores of participants' performance in the subtests of interest; GM: grey matter; HPC: hippocampus; L, R: left, right (hemisphere); rho: Spearmann's rank correlation coefficient; rsFC: resting-state functional connectivity; VBM: voxel-based morphometry.

Figure 3: Visual Recognition Memory: Structural / Functional correlates

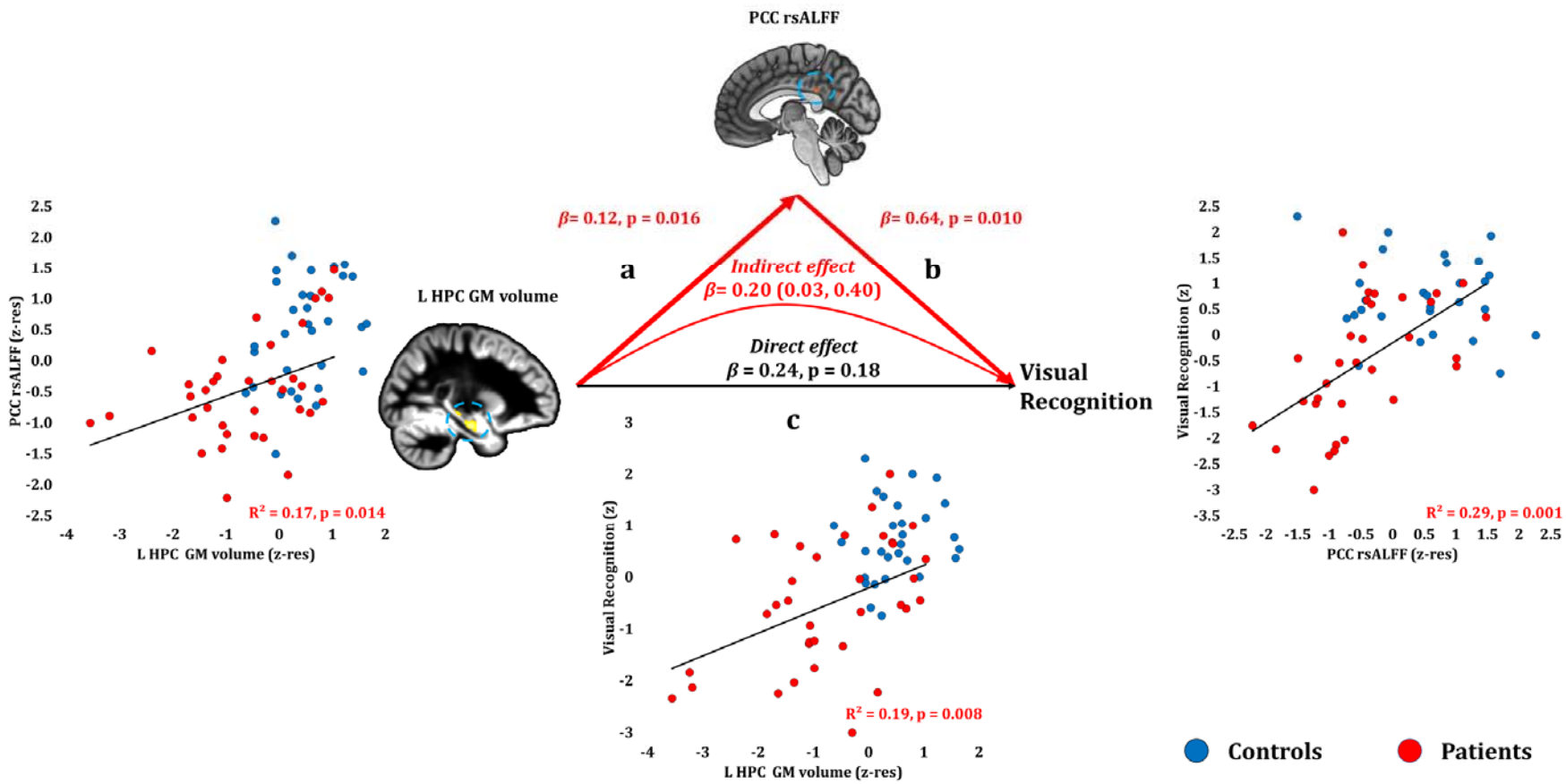

a: mean GM volume of the left HPC cluster correlated with the mean rsALFF of the PCC cluster across patients; b: visual recognition memory scores correlated across patients with their mean rsALFF in the PCC cluster; the mediation analysis demonstrates that this effect held over and above the correlation of PCC rsALFF

with the mean GM volume of the left HPC cluster; c: mean GM volume of the left HPC cluster correlated with visual recognition memory scores across patients; however, the mediation analysis demonstrated that this relationship did not hold over and above the correlation of the mean GM volume of the left HPC cluster with the mean PCC rsALFF; there was only an indirect effect of reduced HPC GM volume on visual recognition memory (within parenthesis: 95% confidence intervals); GM volumes from VBM clusters are residualized against age, sex, and TIV across participants; mean rsALFF values are residualized across participants against age and sex; memory scores are averaged age-scaled and standardized scores of participants' performance in the subtests of interest; GM: grey matter; HPC: hippocampus; L: left (hemisphere); PCC: posterior cingulate cortex; rsALFF: resting-state amplitude of low frequency fluctuations; TIV: total intracranial volume; VBM: voxel-based morphometry.

Figure 4: Verbal Recall Memory: Structural / Functional correlates

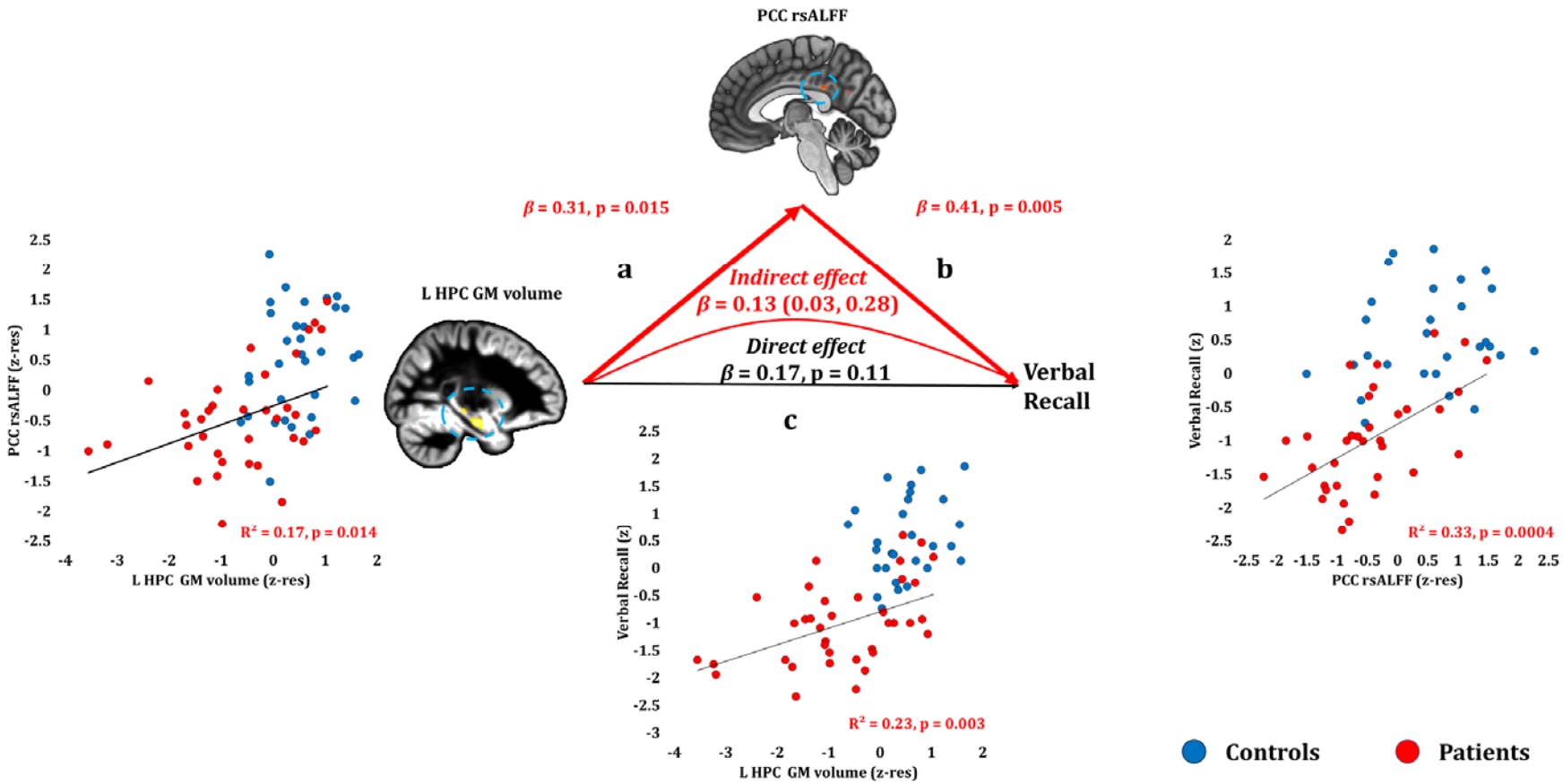

a: mean GM volume of the left HPC cluster correlated with the mean rsALFF of the PCC cluster across patients; b: verbal recall memory scores correlated across patients with their mean rsALFF in the PCC cluster; the mediation analysis demonstrates that this effect held over and above the correlation of PCC rsALFF with the mean GM volume of the left HPC cluster; c: mean GM volume of the left HPC cluster correlated verbal recall memory scores across patients; however, the mediation analysis demonstrated that this relationship did not hold over and above the correlation of the mean GM volume of the left HPC cluster with the mean PCC rsALFF; there was only an indirect effect of reduced HPC GM volume on verbal recall memory (within parenthesis: 95% confidence intervals); GM volumes from VBM clusters are residualized against age, sex, and TIV across participants; mean rsALFF values are residualized across participants against age and sex; memory scores are averaged age-scaled and standardized scores of participants' performance in the subtests of interest; GM: grey matter; HPC: hippocampus; L: left (hemisphere); PCC: posterior cingulate cortex; rsALFF: resting-state amplitude of low frequency fluctuations; TIV: total intracranial volume; VBM: voxel-based morphometry.

Figure 5: Visual Recall Memory: Structural / Functional correlates

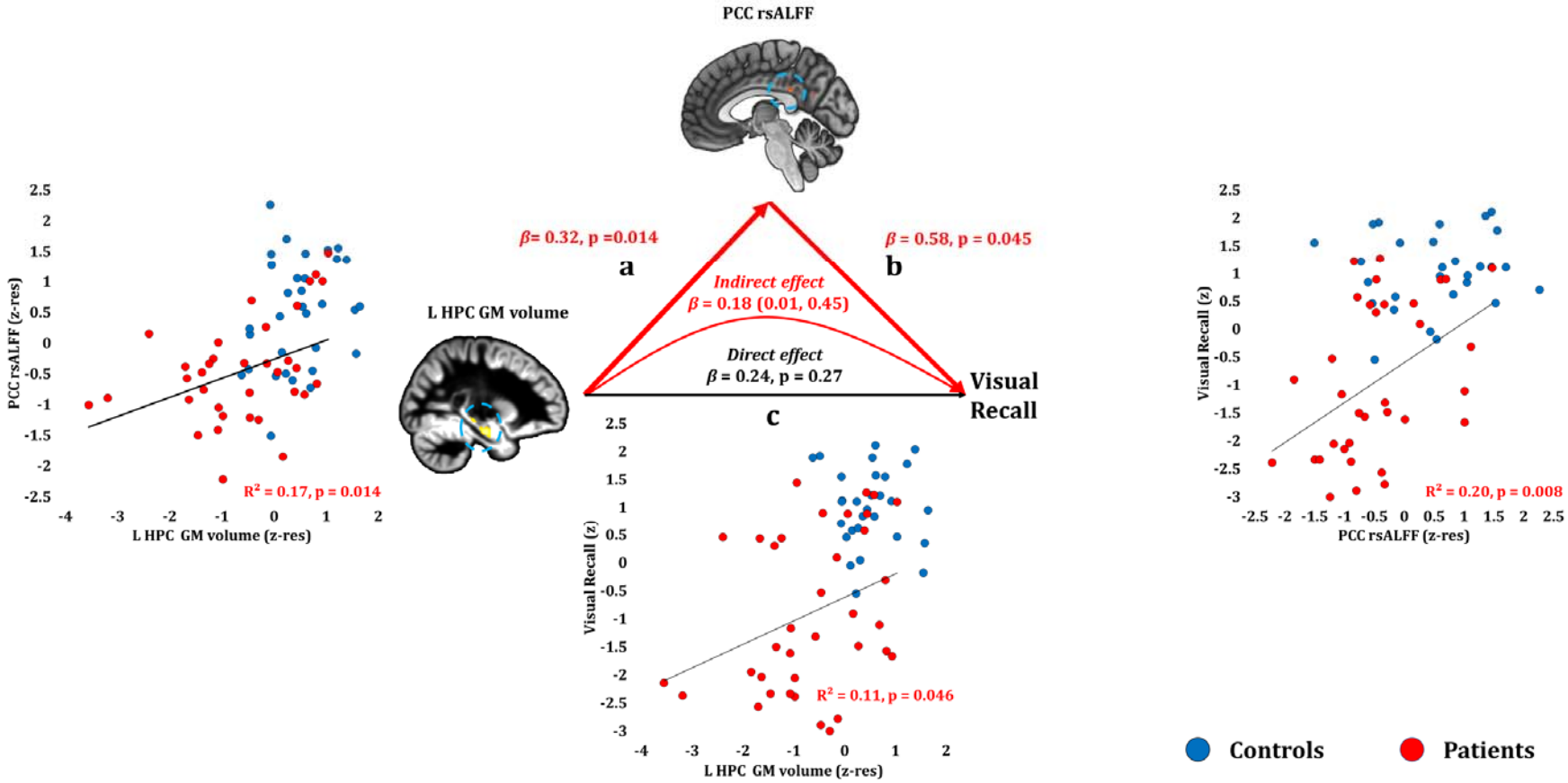

a: mean GM volume of the left HPC cluster correlated with the mean rsALFF of the PCC cluster across patients; b: visual recall memory scores correlated across patients with their mean rsALFF in the PCC cluster; the mediation analysis demonstrates that this effect held over and above the correlation of PCC rsALFF with the mean GM volume of the left HPC cluster; c: mean GM volume of the left HPC cluster correlated with visual recall memory scores across patients; however, the mediation analysis demonstrated that this relationship did not hold over and above the correlation of the mean GM volume of the left HPC cluster with the mean PCC rsALFF; there was only an indirect effect of reduced HPC GM volume on visual recall memory (within parenthesis: 95% confidence intervals); GM volumes from VBM clusters are residualized against age, sex, and TIV across participants; mean rsALFF values are residualized across participants against age and sex; memory scores are averaged age-scaled and standardized scores of participants' performance in the subtests of interest; GM: grey matter; HPC: hippocampus; L: left (hemisphere); PCC: posterior cingulate cortex; rsALFF: resting-state amplitude of low frequency fluctuations; TIV: total intracranial volume; VBM: voxel-based morphometry.

Figure 6: Visual Forgetting: Structural / Functional correlates

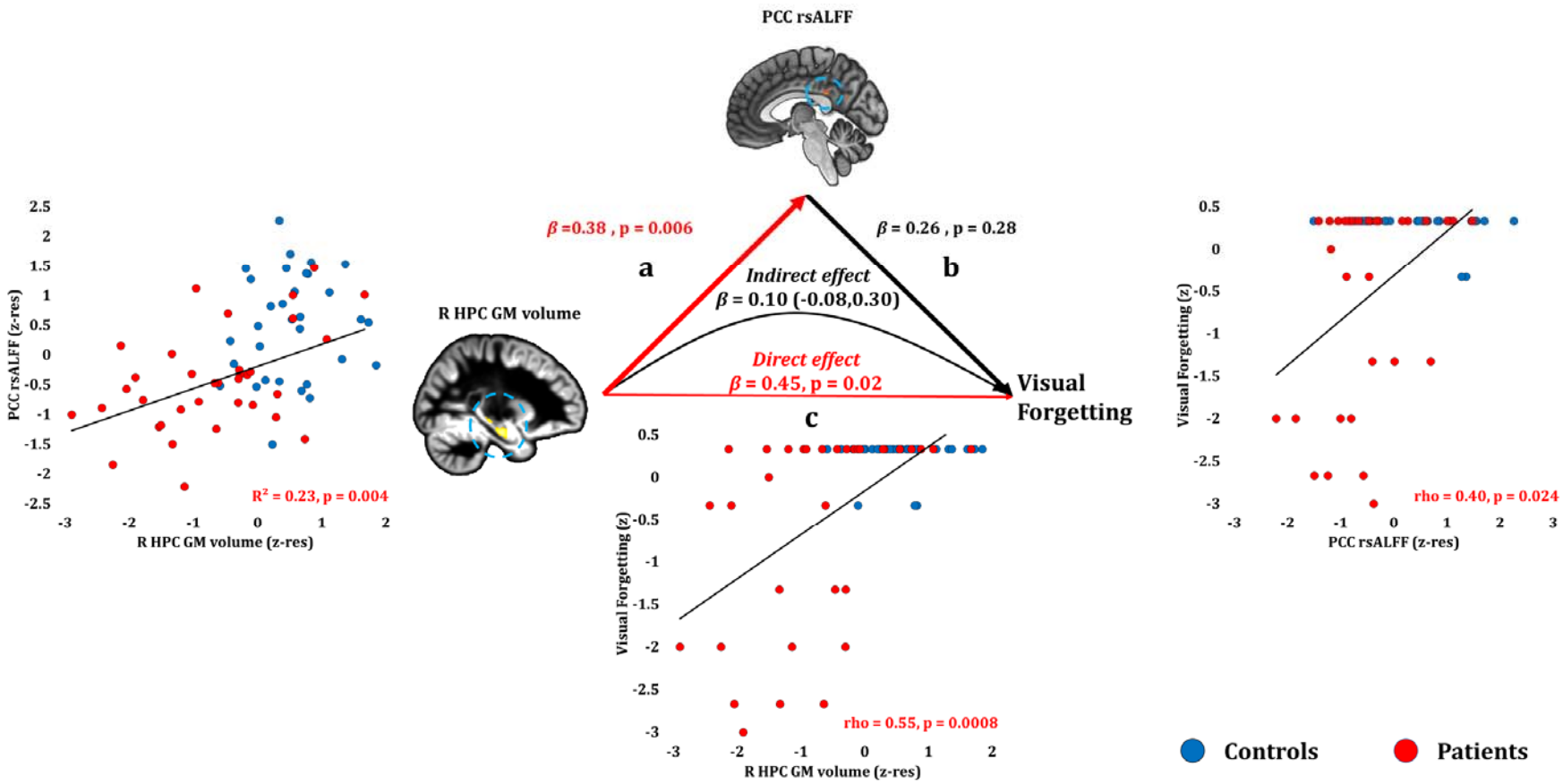

a: mean GM volume of the right HPC cluster correlated with the mean rsALFF of the PCC cluster across patients; b: visual forgetting scores correlated across patients with their mean rsALFF in the PCC cluster; the mediation analysis demonstrates that this effect did not hold when the correlation of PCC rsALFF with the mean GM volume of the right HPC cluster was accounted for; c: mean GM volume of the right HPC cluster correlated with visual forgetting scores across patients; the mediation analysis demonstrated that this relationship held over and above the correlation of the mean GM volume of the right HPC cluster with the mean PCC rsALFF; there was thus a direct effect of reduced HPC GM volume on visual forgetting (within parenthesis: 95% confidence intervals); GM volumes from VBM clusters are residualized against age, sex, and TIV across participants; mean rsALFF values are residualized across participants against age and sex; memory scores are averaged age-scaled and standardized scores of participants' performance in the subtests of interest; GM: grey matter; HPC: hippocampus; PCC: posterior cingulate cortex; R: right (hemisphere); rsALFF: resting-state amplitude of low frequency fluctuations; TIV: total intracranial volume; VBM: voxel-based morphometry.

Figure 7: Remote Autobiographical Memory: Structural / Functional correlates

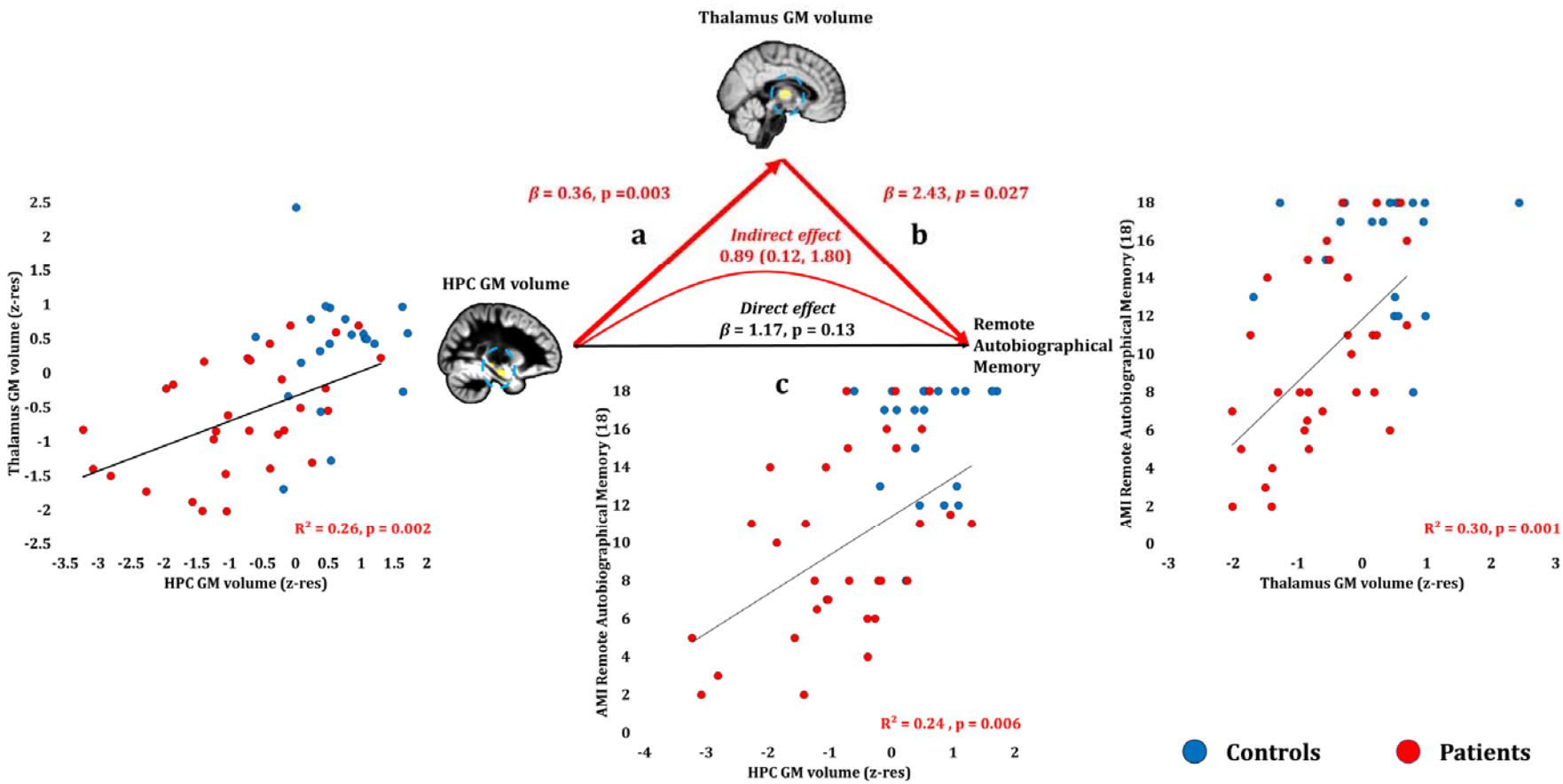

a: mean GM volume of the two HPC clusters correlated with the mean GM volume of the three thalamic clusters across patients; b: remote autobiographical memory (AMI) scores correlated across patients with the mean GM volume of the three thalamic clusters; the mediation analysis demonstrates that this effect held when the correlation of thalamic GM volume with the mean GM volume of the HPC clusters was accounted for; c: mean GM volume of the HPC clusters correlated with remote autobiographical memory scores; the mediation analysis demonstrated that this relationship did not hold over and above the correlation of the mean GM volume of the thalamic clusters with the HPC clusters; there was thus no direct effect of reduced HPC GM volume on remote autobiographical memory (within parenthesis: 95% confidence intervals); GM volumes from VBM clusters are residualized against age, sex, and TIV across participants; remote autobiographical memory scores are the sums of the AMI scores for autobiographical memories for childhood and early adulthood (max = 18); AMI: Autobiographical Memory Interview; GM: grey matter; HPC: hippocampus; TIV: total intracranial volume; VBM: voxel-based morphometry.